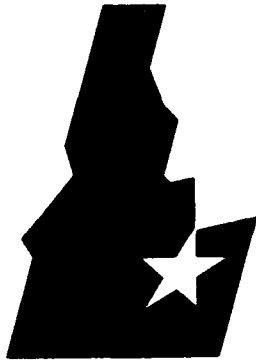


DTIC FILE COPY

1

EGG-MS-8945
March 1990



**Idaho
National
Engineering
Laboratory**

INFORMAL REPORT

INVESTIGATION OF WELD BEAD
COOLING RATE DURING STARTUP
OF GAS METAL ARC WELDING

*Managed
by the U.S.
Department
of Energy*

H. B. Smartt
H. L. Brown
R. A. Morris

AD-A223 567

Approved for public release;
distribution is unlimited.

DTIC
ELECTE
JUN 29 1990
S B D
Cc



*Work performed under
DOE Contract
No. DE-AC07-76ID01570*

90 06 28 061

DISCLAIMER

This book was prepared as an account of work sponsored by an agency of the United States Government. Neither the United States Government nor any agency thereof, nor any of their employees, makes any warranty, express or implied, or assumes any legal liability or responsibility for the accuracy, completeness, or usefulness of any information, apparatus, product or process disclosed, or represents that its use would not infringe privately owned rights. References herein to any specific commercial product, process, or service by trade name, trademark, manufacturer, or otherwise, does not necessarily constitute or imply its endorsement, recommendation, or favoring by the United States Government or any agency thereof. The views and opinions of authors expressed herein do not necessarily state or reflect those of the United States Government or any agency thereof.

REPORT DOCUMENTATION PAGE

1a REPORT SECURITY CLASSIFICATION Unclassified		1b RESTRICTIVE MARKINGS N/A	
2a SECURITY CLASSIFICATION AUTHORITY N/A		3 DISTRIBUTION/AVAILABILITY OF REPORT Approved for public release; distribution is unlimited	
2b DECLASSIFICATION/DOWNGRADING SCHEDULE N/A		4 PERFORMING ORGANIZATION REPORT NUMBER(S) EGG-MS-8945	
4 PERFORMING ORGANIZATION REPORT NUMBER(S) EGG-MS-8945		5 MONITORING ORGANIZATION REPORT NUMBER(S)	
6a NAME OF PERFORMING ORGANIZATION Idaho National Engineering Laboratory	6b OFFICE SYMBOL (If applicable)	7a NAME OF MONITORING ORGANIZATION David Taylor Research Center	
6c ADDRESS (City, State, and ZIP Code) P.O. Box 1625 Idaho Falls, ID 83415-2210		7b ADDRESS (City, State, and ZIP Code) Code 2815 Annapolis, MD 21402-5067	
8a NAME OF FUNDING/SPONSORING ORGANIZATION OCNR 225	8b OFFICE SYMBOL (If applicable)	9. PROCUREMENT INSTRUMENT IDENTIFICATION NUMBER N00167-88-WR8-0059	
8c ADDRESS (City, State, and ZIP Code) 800 N. Quincy Street Arlington, VA 22217		10 SOURCE OF FUNDING NUMBERS	
		PROGRAM ELEMENT NO 62761N	PROJECT NO
		TASK NO	WORK UNIT ACCESSION NO
11 TITLE (Include Security Classification) Investigation of Weld Bead Cooling Rate During Startup of Gas Metal Arc Welding (Unclassified)			
12 PERSONAL AUTHOR(S) H. B. Smartt, H. L. Brown, R. A. Morris			
13a TYPE OF REPORT Annual	13b TIME COVERED FROM 10/88 TO 9/89	14 DATE OF REPORT (Year, Month, Day) 1990, March	15 PAGE COUNT 49
16 SUPPLEMENTARY NOTATION			
17 COSATI CODES		18 SUBJECT TERMS (Continue on reverse if necessary and identify by block number)	
FIELD	GROUP	Welding, Controls, Sensing	
19 ABSTRACT (Continue on reverse if necessary and identify by block number) Most rejectable gas metal arc weld defects occur during weld initiation. Such defects are probably caused by nonequilibrium thermal conditions during weld startup which result in higher than normal weld bead cooling rates. This report describes experimental studies to investigate the feasibility of decreasing the initial weld bead cooling rate. A control model that allows independent setting of weld heat and mass input was used in combination with a proportional-integral controller. Startup and steady-state weld bead cooling rates have been established for a range of heat inputs. The controller was then used to delay welding torch movement for 4 s, and to apply a higher than normal heat input during the first 7 s of the weld. Heat input was then reduced to a predetermined lower value while maintaining constant mass input. The combination of delayed torch movement and 12.5% higher initial heat input reduced the weld bead cooling rate by at least 40% during weld startup. Present results confirm the feasibility of modifying the initial weld bead cooling rate by appropriate combinations of equipment operating parameters, but an extra heat source is needed to achieve an initial cooling rate equal to the subsequent steady-state rate. (25) 15			
20 DISTRIBUTION/AVAILABILITY OF ABSTRACT <input type="checkbox"/> UNCLASSIFIED UNLIMITED <input checked="" type="checkbox"/> SAME AS RPT <input type="checkbox"/> DTIC USERS		21 ABSTRACT SECURITY CLASSIFICATION Unclassified	
22a NAME OF RESPONSIBLE INDIVIDUAL Richard A. Morris		22b TELEPHONE (Include Area Code) (301) 267-3548	22c OFFICE SYMBOL DTRC, Code

CONTENTS

ABSTRACT.....	i
INTRODUCTION.....	1
APPROACH.....	2
Concept.....	2
Model.....	2
Filter.....	9
Welding Hardware.....	11
Controller.....	11
EXPERIMENTAL STUDIES.....	13
Controller Gains.....	13
Constant Heat Input Cooling Rate.....	27
Stepped Heat Input Cooling Rate.....	30
Delayed-Start Stepped Heat Input Cooling Rate.....	33
Arc Initiation.....	35
RESULTS AND CONCLUSIONS.....	38
REFERENCES.....	40

FIGURES

1. Schematic diagram of computer-controlled GMA welding machine	3
2. Operator's panel and computer for computer-controlled GMA welding machine	4
3. Welding head for computer-controlled GMA welding machine	5
4. Cut-away drawing of gas metal arc welding torch	5
5. Gas metal arc process spray transfer mode region as a function of heat input per length of weld and reinforcement area	10
6. Feedback control scheme for independent control of weld bead reinforcement area and heat input per length of weld	12
7. Measured current and voltage as a function of time for a weld (T10) made using a poor set of controller gains	14

8.	Measured current and voltage as a function of time for a weld (T22) made using a good set of controller gains	15
9.	Digitized current as a function of time for weld T10	16
10.	Current as a function of time for weld T10, filtered with a 1 Hz Butterworth low-pass filter	16
11.	Current as a function of time for weld T10, as measured by the computer-controlled GMA welding machine	17
12.	Model-calculated current as a function of time for weld T10	17
13.	Controller error signal as a function of time for weld T10	18
14.	Model-calculated CT as a function of time for weld T10	18
15.	Electrode wire speed as a function of time for weld T10	19
16.	Welding speed as a function of time for weld T10	19
17.	Calculated heat input per length of weld for weld T10	20
18.	Calculated reinforcement as a function of time for weld T10	20
19.	Digitized current as a function of time for weld T22	22
20.	Current as a function of time for weld T22, filtered with a 1 Hz Butterworth low-pass filter	22
21.	Current as a function of time for weld T22, as measured by the computer-controlled GMA welding machine	23
22.	Model-calculated current as a function of time for weld T22	23
23.	Controller error signal as a function of time for weld T22	24
24.	Model-calculated CT as a function of time for weld T22	24
25.	Electrode wire speed as a function of time for weld T22	25
26.	Welding speed as a function of time for weld T22	25
27.	Calculated heat input per length of weld for weld T22	26
28.	Calculated heat input per length of weld for weld T36	28
29.	Calculated heat input per length of weld for weld T37	28
30.	Calculated heat input per length of weld for weld T41	29

31.	Calculated heat input per length of weld for weld T46	29
32.	Weld bead cooling rate at 1000°F as a function of heat input per length of weld	31
33.	Calculated heat input per length of weld for weld T60	31
34.	Calculated heat input per length of weld for weld T62	32
35.	Calculated heat input per length of weld for weld T63	32
36.	Weld bead cooling rate at 1000°F as a function of distance from start of bead, for 1800/1480 J/mm stepped heat input.....	33
37.	Weld bead cooling rate at 1000°F as a function of distance from start of bead, for 1800/1600 J/mm stepped heat input and 4s delayed start.....	34



Accession For	
NTIS GRA&I	<input checked="" type="checkbox"/>
DTIC TAB	<input type="checkbox"/>
Unannounced	<input type="checkbox"/>
Justification _____	
By _____	
Distribution/ _____	
Availability Codes	
Dist	Avail and/or Special
A-1	

INVESTIGATIONS OF WELD BEAD COOLING RATE
DURING STARTUP OF GAS METAL ARC WELDING

INTRODUCTION

Experience in fabrication of steel structures using the automated gas metal arc welding (GMA or GMAW) process has shown that most rejectable weld defects occur in the first portion of weld bead deposited during welding. Two aspects of the welding process appear to contribute to this situation. One, it takes a finite period of time (~ 0.1 s) for the arc to stabilize and equilibrium electrode wire melting to establish. Two, even joining of preheated base plates requires a relatively long period of time (~ 10 s) for quasi-steady-state weld pool and bead cooling rates to develop. Given the above, it is postulated that a reasonable strategy for reducing weld defects may be based on an approach which brings the electrode wire melting process to equilibrium as soon as possible and equilibrates the weld pool/bead cooling rate as soon as possible during startup of the welding process.

The objective of this work is to conduct a feasibility study to determine if it is practical to weld with the GMA process in a manner in which the weld heat input is deliberately maintained at a relatively high level during weld startup and then reduced to the steady-state level while simultaneously maintaining a constant mass input to the weld pool. As part of this study, the weld bead cooling rate is measured to determine if the above procedure will allow nominal steady-state weld bead cooling rates to be achieved during weld startup. The feasibility of this approach is supported by the modeling work of Ule,¹ which shows that steady-state thermal behavior for a weld can be reached more quickly by increasing the initial heat input.

APPROACH

The discussion is organized in terms of the concept behind the work, the control model and controller, the hardware used, and the experimental results and conclusions.

Concept

The work is based on the use of a computer-controlled laboratory prototype, automated gas metal arc welding system described previously,² and shown schematically in Figure 1. The computer and operator panel are shown in Figure 2, and the weld head and table are shown in Figure 3. This system employs a model-based adaptive feedback control scheme that allows the heat input (per length of weld) and the mass input (in terms of weld bead reinforcement area) to be specified and controlled independently over the normal range of operating parameters. The model and control scheme are described in the following sections.

In this work, welds are made using the above system to maintain weld heat and mass input constant; the resulting weld bead cooling rate is measured in the initial weld pool formed and after the process has attained quasi-steady-state operating conditions. Welds are also made during which the mass input is maintained constant but the weld heat input is deliberately maintained at a higher than normal value during the first portion of the weld and then dropped to the normal value. In this work, "normal" is based on obtaining spray transfer³ of the filler metal from the electrode to the weld pool.

Model

The GMAW process employs a consumable electrode passing through a copper alloy contact tip (Figure 4). Electrical current, imposed on the wire by a voltage drop between the contact tip and the metal to be welded (base metal), supports an arc between the wire end and the base metal. The electrode is melted by internal resistive power and heat transferred from the arc. Droplets of molten metal are detached and transferred from the the

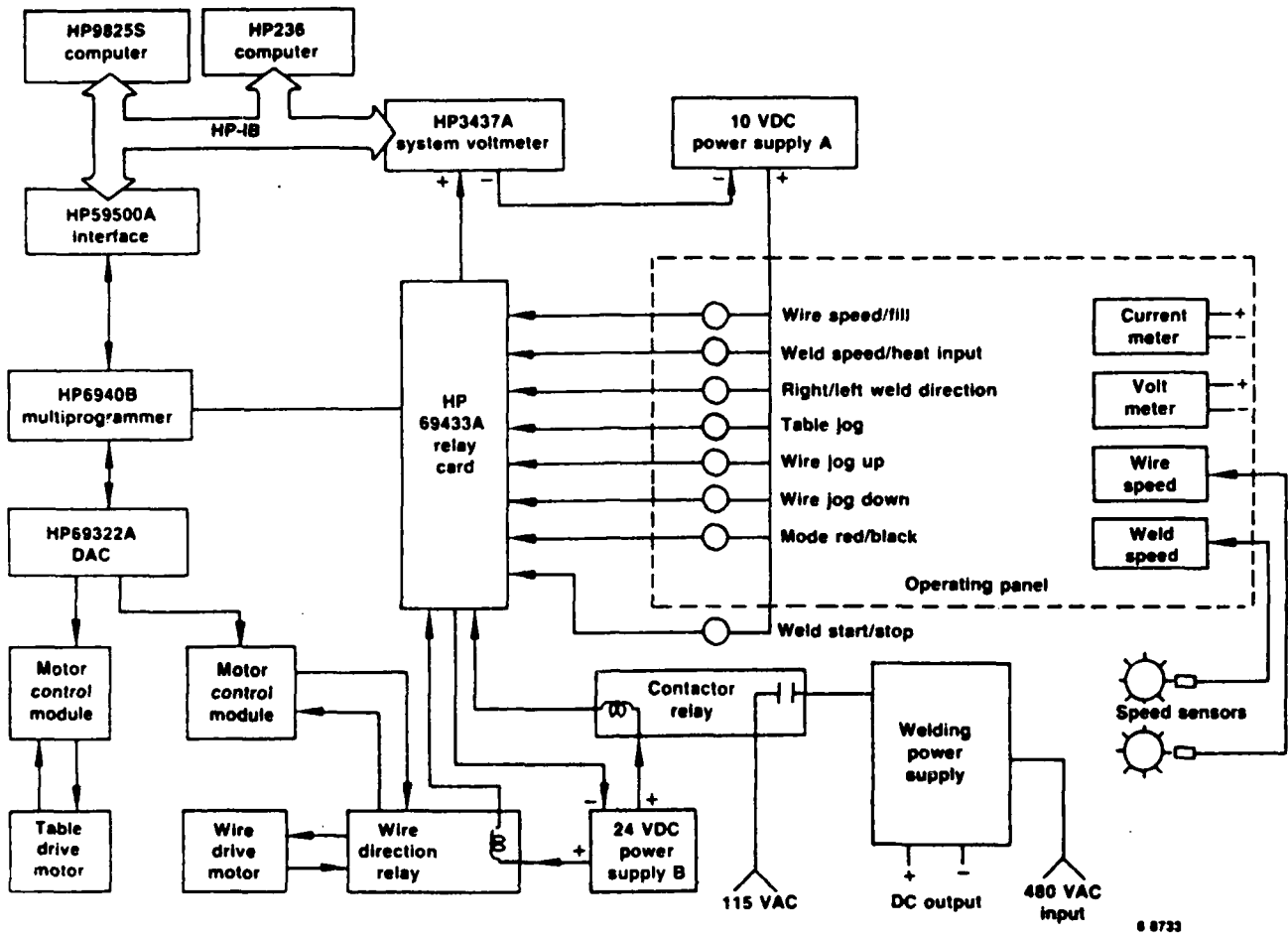


Figure 1. Schematic diagram of computer-controlled GMA welding machine.

wire to the weld pool by the combination of gravitational, Lorentz, surface tension, and plasma forces.³ Heat is transferred to the base metal directly from the arc and by the molten metal droplets. The electrode wire, molten droplets, weld pool, and the solidified weld bead behind the weld pool are protected from oxidation by a shielding gas which may be Ar, CO₂, or mixtures such as Ar with O₂, H₂, He, or CO₂ in various combinations. The process may be performed with the electrode wire at a positive or a negative potential with respect to the base metal, using either a constant current or a constant voltage power supply, with either pulsed or constant electrode wire speed and/or welding current. However, the most common operating conditions are for electrode wire positive, using a constant voltage power supply, with constant wire speed and current. This work is limited to such conditions.

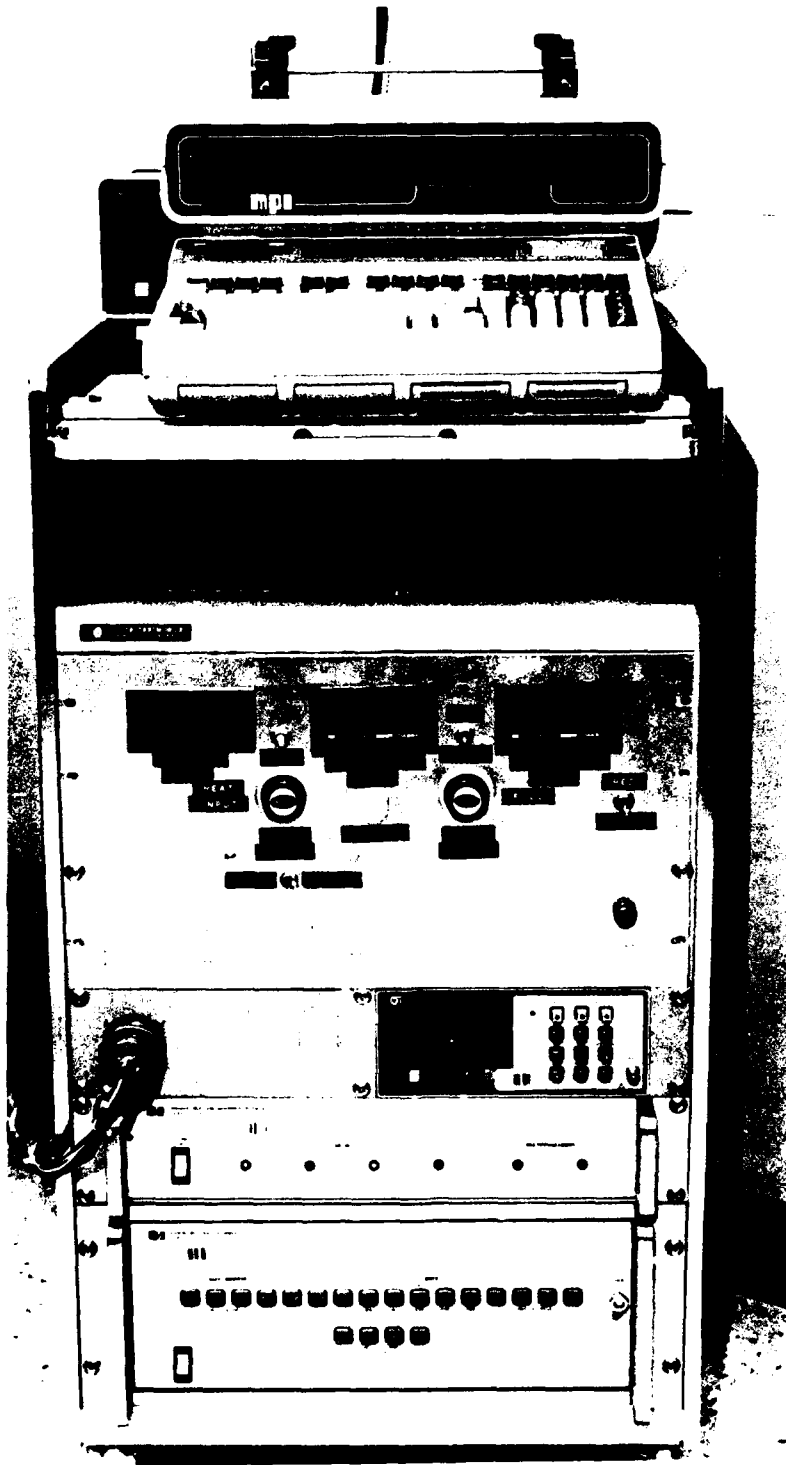


Figure 2. Operator's panel and computer for computer-controlled GMA welding machine.

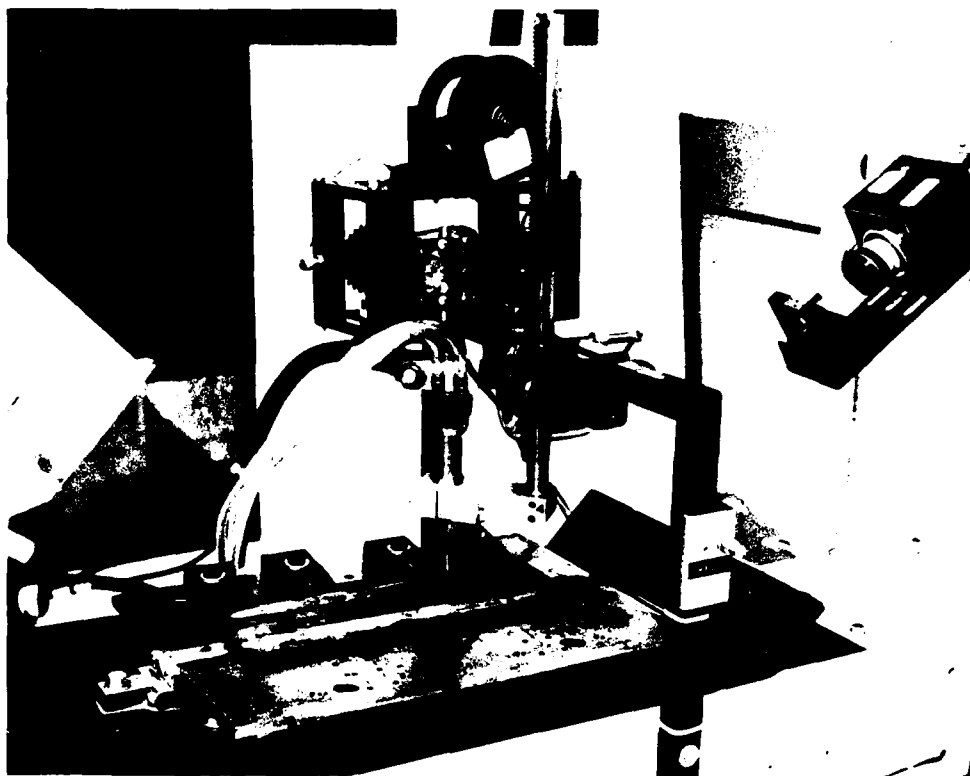
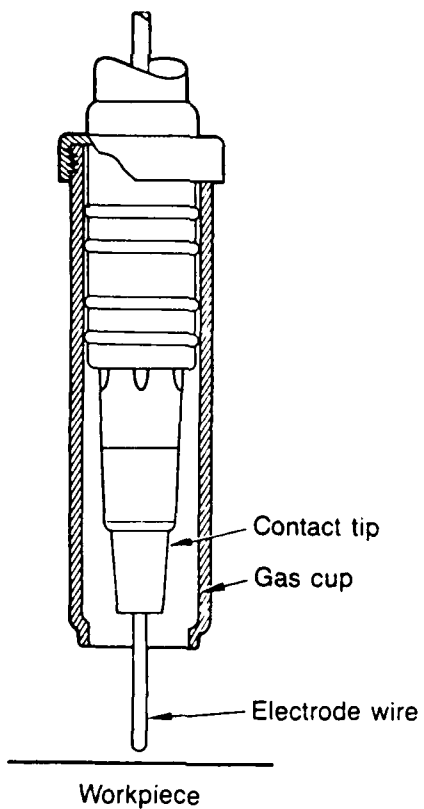


Figure 3. Welding head for computer-controlled GMA welding machine.



6 12 985

Figure 4. Cut-away drawing of gas metal arc welding torch.

The heat input (H) to the base metal per unit length of weld is given by:

$$H = EI\eta/R \quad (1)$$

where

E = voltage

I = current

R = welding speed

η = heat transfer efficiency.

The weld bead reinforcement (G), defined as the transverse cross-sectional area of the deposited metal, is given by:

$$G = (S/R)d^2\pi/4 \quad (2)$$

where

S = filler wire speed

d = wire diameter.

The output voltage of the power supply (E) is given by:

$$E = E_0 + nI + L \frac{dI}{dt} \quad (3)$$

where

E_0 = the open circuit voltage of the supply (i.e., at zero load)

n = the effective slope of the supply (i.e., the combined effects of power supply slope and secondary circuit resistance)

L = power supply secondary circuit inductance

t = time.

Current is maintained by the power supply consistent with the contact-tip-to-base-metal resistance, which is determined by the wire stickout and arc resistance, and the contact-tip-to-base-metal voltage. Power consumed by the process is the sum of that consumed by resistive heating of the electrode wire and that consumed in the arc as:

$$IE = IV_w + IV_a \quad (4)$$

where V_w is the voltage drop along the electrode wire and V_a is the voltage drop across the arc. The power required to melt the electrode wire is given by:

$$IV_w + \eta' IV_a = \delta S H_m d^2 \pi / 4 \quad (5)$$

where

η' = efficiency of heat transfer from the arc to the electrode wire

δ = density

H_m = heat required to melt a unit volume of material, given as:

$$H_m = \int_{T_0}^{T_m} C_p dT + H_f \quad (5')$$

where

C_p = the specific heat

T_0 and T_m are the ambient and melting temperatures

H_f = the heat of fusion.

Finally, Ohm's law is used:

$$IV_a = I^2 R_a \quad (6)$$

to determine power consumption in the arc, where R_a is the arc resistance and both sides of Equation (6) are multiplied by the current. In normal operation of the process, the welding current is controlled by changing the wire speed. The amount of fill (reinforcement area) is controlled by changing the welding speed. The net result is that normally the heat input to the weld and the mass input to the weld are not controlled independently. Yet, such independence can be obtained by solving the above Equations (1)-(6), appropriately.

It can be shown that:

$$S = \frac{E_o \eta 4GI + n\eta 4GI^2}{\pi d^2 H} \quad (7)$$

and

$$R = \frac{S\pi d^2}{4G} \quad (8)$$

where

S = the wire speed

R = the welding speed

G = the reinforcement area

H = the heat input per length of weld.

The fact that a steady-state model can be used is due to the relatively short time constant associated with the electrical system and the sufficiently high (although under-damped) damping associated with the thermal problem. The current (I) is given by:

$$I = C_0 + C_1 \cdot CT + C_2 \cdot E_0 + C_3 \cdot S \quad (9)$$

where the C terms are constants.

The above Equations (7)-(9) may be solved iteratively.

The above analysis contains no information on the detachment of liquid metal drops from the electrode wire. Droplet detachment is controlled by current-driven pinch-off of the liquid metal column on the end of the electrode wire. A discussion of droplet detachment has been given by Waszink and Piena.⁴

The process operating range may be shown to lie within the heat input/reinforcement domain. Figure 5 presents such an operating range for carbon steel wire and base metal, Ar-O₂ shield gas, and certain other conditions which may affect the position of the operating range in the domain. Several points should be noted. The left side boundary of the operating region corresponds to the limiting case where V_a goes to zero; in this case the electrode wire stubs into the weld pool. The right side boundary corresponds to the limiting case where V_w goes to zero; in this case the arc transfers to the contact tip. The intermediate boundary corresponds to the transition from globular to spray transfer of drops from the electrode wire to the weld pool. Other possible modes of such transfer are not discussed in detail here. (The reader may see Lancaster³ for a more complete description.) In simple terms, gravity is the major force driving droplet transfer in the globular mode, while the electromagnetic force is the major force driving droplet transfer in the spray mode.

Filter

The current is measured by the system during welding by obtaining the voltage drop across a calibrated shunt placed in the secondary current loop. The resulting signal is very noisy, having about a ± 1 to 10 A peak-to-peak variation, which is too great to allow direct measurement of the voltage to be useful for controlling the process. To overcome this problem this work employs a digital filter in the time domain.

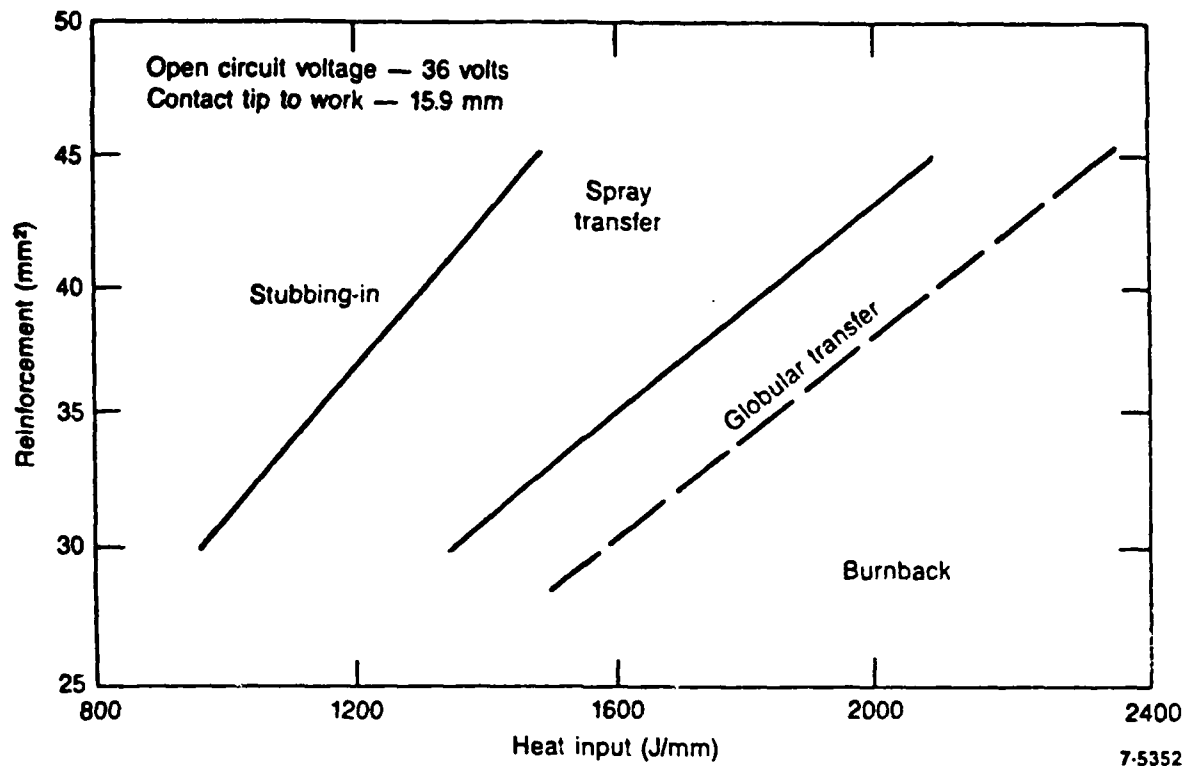


Figure 5. Gas metal arc process spray transfer mode region as a function of heat input per length of weld and reinforcement area.

The shunt voltage is measured in sets of 30 values taken at the rate of 3600/s. The last 20 of these values are processed by a simple finite impulse response filter:⁵

$$Y(t) = \sum_{i=10}^{30} h_i X_i \quad (10)$$

where $h_i = 0.05$. Thus, $Y(t)$ is the average of 20 data points (X_i) taken approximately at time t . The first ten values are discarded to remove any artifacts associated with the relay switching used for multiplexing. At approximately one-half-second intervals, the present and the last two $Y(t)$ values are processed using a simple infinite impulse response filter:⁵

$$Z(t) = CY_0 + \sum_{i=-2}^{-1} b_i Z_i \quad (11)$$

where $C = 0.5$ and $b_i = 0.25$. Thus, $Z(t)$ is a weighted, moving average.

Welding Hardware

The gas metal arc welding system developed for this work consists of a computer-controlled welding head, positioning table, and an operator panel which is the front end for a Philips transistorized 460 A welding power supply operating at a switching frequency of 40 kHz, in a constant-voltage mode. In operation, the desired levels of weld bead reinforcement area (fill) and heat input per length of weld are set on the operating panel in engineering units of mm^2 and J/mm , respectively. The system then controls the electrode wire speed and welding speed, based on the model solutions, to give the desired values.

Controller

In the process control scheme, the difference between measured current (filtered) and calculated current is used as the error signal input (e) to a proportional-integral-derivative (PID) controller which calculates the value of the parameter (CT) corresponding to the contact-tip-to-workpiece distance in Equation (9):

$$CT(t) = K_p e(t) + K_i \int_{t_0}^t e(t) dt + K_d de(t)/dt \quad (12)$$

where K_p , K_i , and K_d are the controller proportional, integral, and derivative gains respectively, but in this work K_d is zero. The integral error is calculated using Simpson's rule. Thus, the value of CT is continuously adjusted to reduce the difference between measured and calculated current. The maximum change in the parameter CT is limited to ± 10 mm at any time; this allows welding with globular metal transfer. The corresponding control system block diagram is shown in Figure 6.

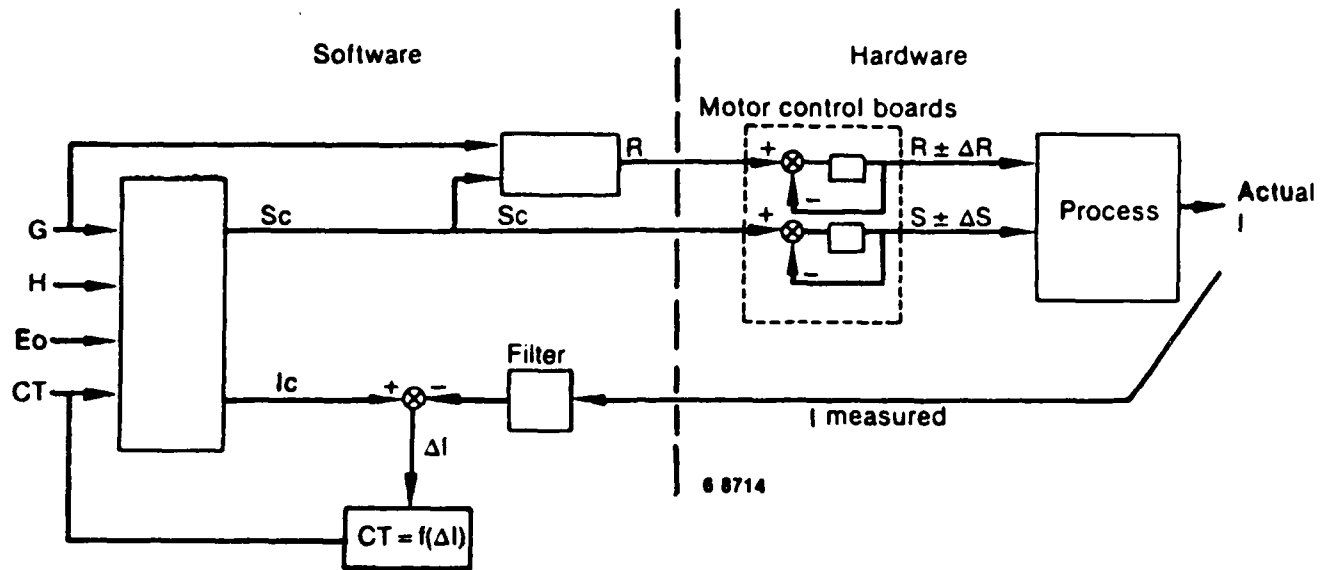


Figure 6. Feedback control scheme for independent control of weld bead reinforcement area and heat input per length of weld.

EXPERIMENTAL STUDIES

A series of 87 welds (designated T01 to T87) was made, using the model to control reinforcement area and heat input with 0.89 mm (0.035 in.) diameter type E70S-6 wire, Ar-20₂ shielding gas, on 12.7 mm (1/2 in.) thick type A-36 steel plate in a bead-on-plate configuration. Welds designated T01 to T63 were made with nominal 95°F (35°C) preheat temperature; subsequent welds were made with nominal 110°F (41.7°C) preheat temperature. Weld bead cooling rates were measured using Type K thermocouples plunged into the weld pool at the top center of the weld bead. A majority of the welds was made to determine the optimum controller gains, identify realistic test parameters, and obtain valid thermocouple data. Thus data are not shown for all 87 welds in this report. Data were also taken on weld current measurements to evaluate alternative filter designs. In addition, a video tape showing most of the welds was made using a weld vision system described elsewhere.² This tape is available from the authors.

Controller Gains

Welds through T22 were made to evaluate the effects of changing the proportional and derivative gains in Equation (12). For example, Figure 7 shows current and voltage measurements made on a HP 7132A strip chart recorder during a weld (T10) made with a heat input of 1600 J/mm, reinforcement area of 40.4 mm², $K_p = 0.01$ and $K_i = 0.05$ with changes in CT limited to ± 2 mm; the amount of overshoot and steady-state error in the current shown is not acceptable. Indeed, during most of weld T10 metal transfer was globular. In contrast, T22 (Figure 8) shows a stable process startup with spray transfer of metal under similar conditions with gains of $K_p = 0.07$ and $K_i = 0.05$ and changes in CT limited to ± 10 mm. The values used in T22 were employed for all subsequent welds.

Figures 9 through 18 illustrate the behavior of the controller during weld T10 in more detail. In Figure 9, the weld current is shown, taken at a digitizing rate of 250 Hz; the same data are shown in Figure 10 after having been filtered by a low-pass, first-order Butterworth filter with a 1 Hz

Current

Voltage

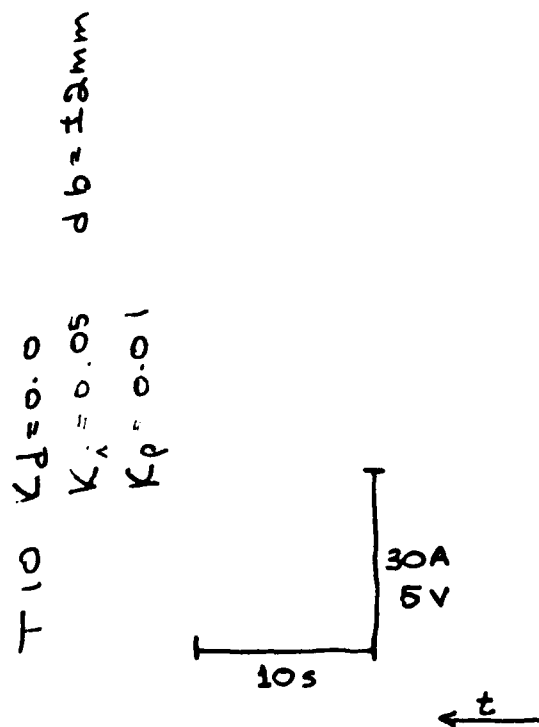


Figure 7. Measured current and voltage as a function of time for a weld (T10) made using a poor set of controller gains.

Current

Voltage

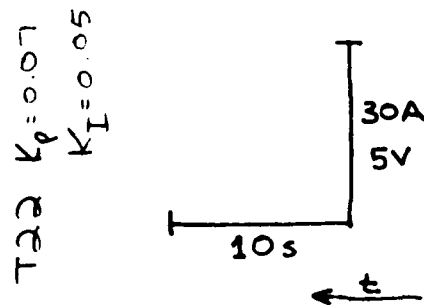


Figure 8. Measured current and voltage as a function of time for a weld (T22) made using a good set of controller gains.

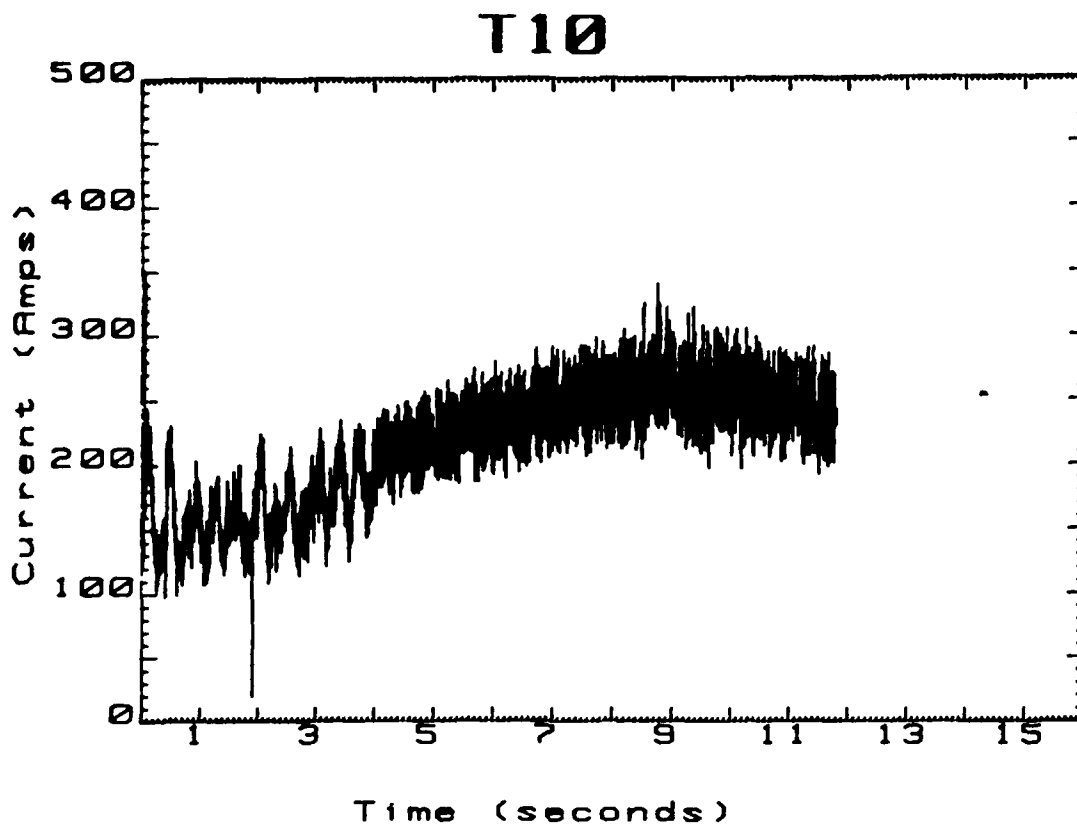


Figure 9. Digitized current as a function of time for weld T10.

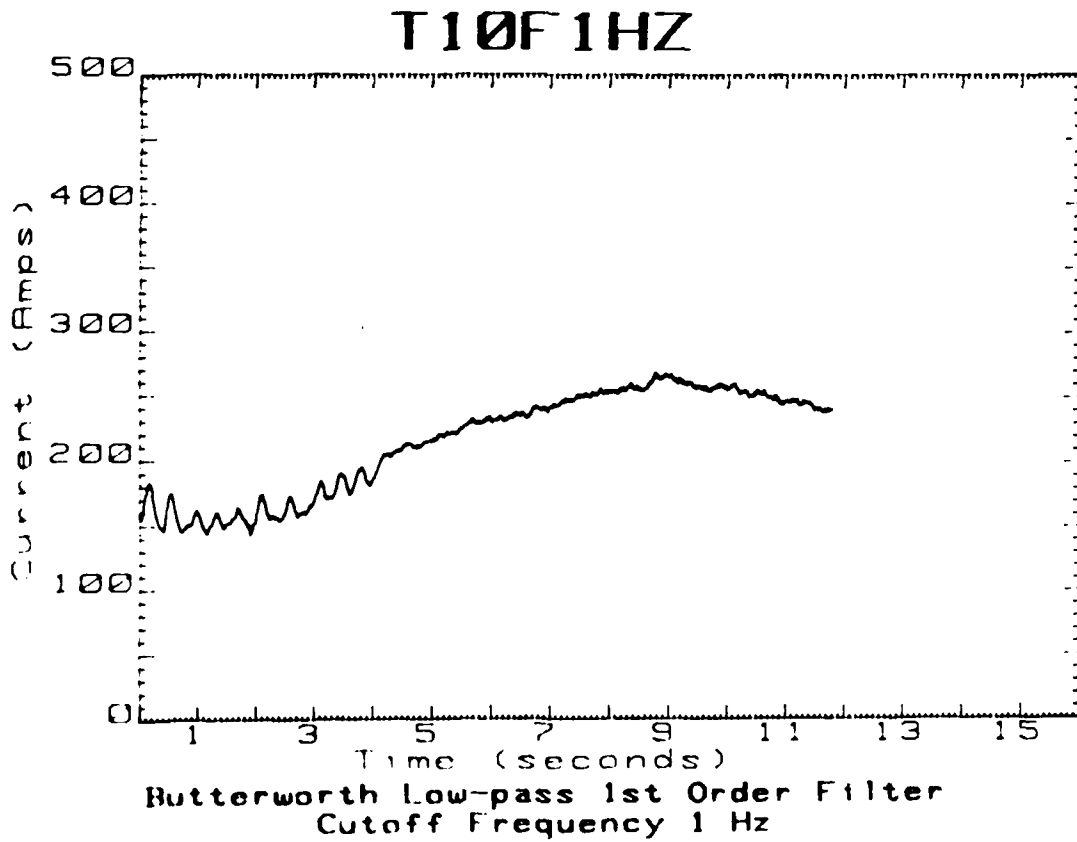


Figure 10. Current as a function of time for weld T10, filtered with a 1 Hz Butterworth low-pass filter.

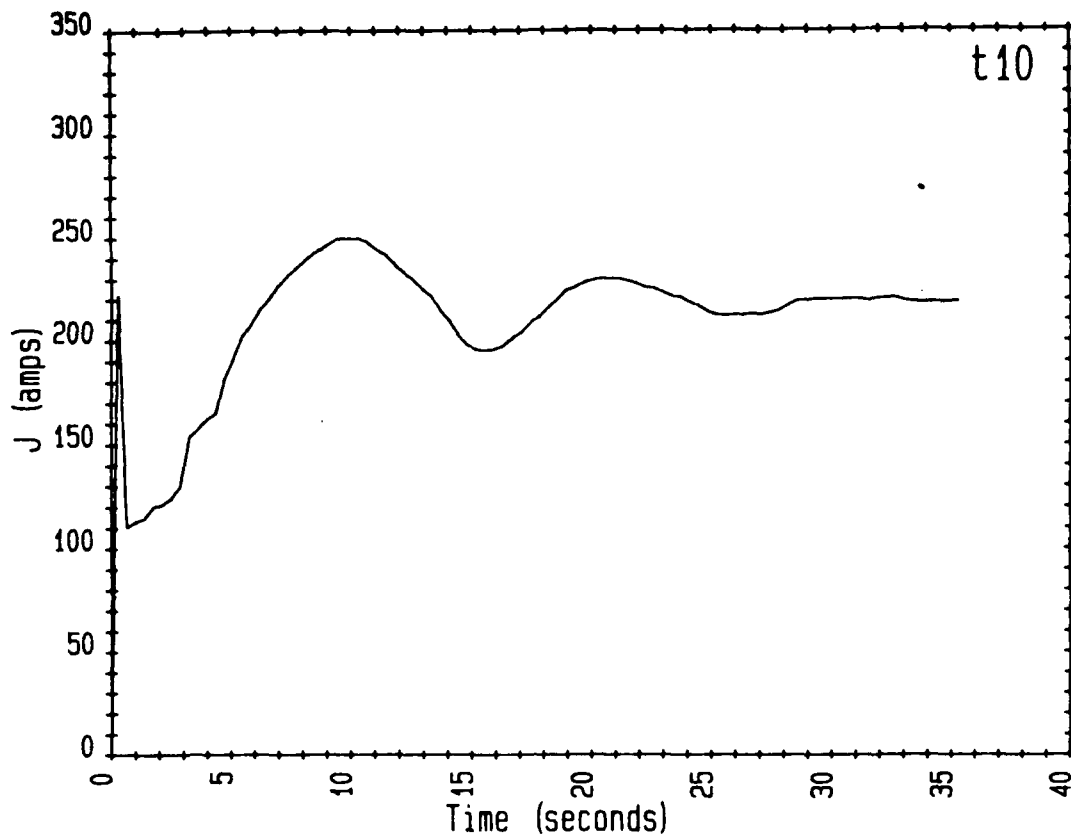


Figure 11. Current as a function of time for weld T10, as measured by the computer-controlled GMA welding machine.

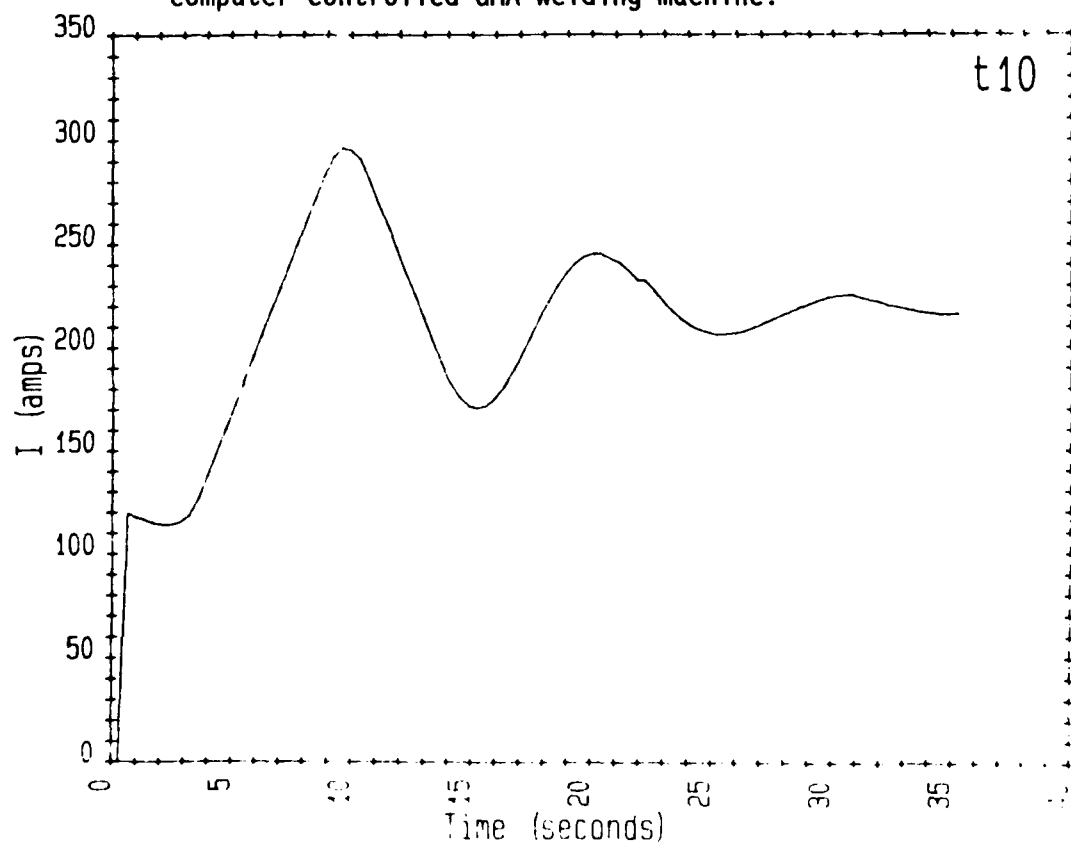


Figure 12. Model-calculated current as a function of time for weld T10.

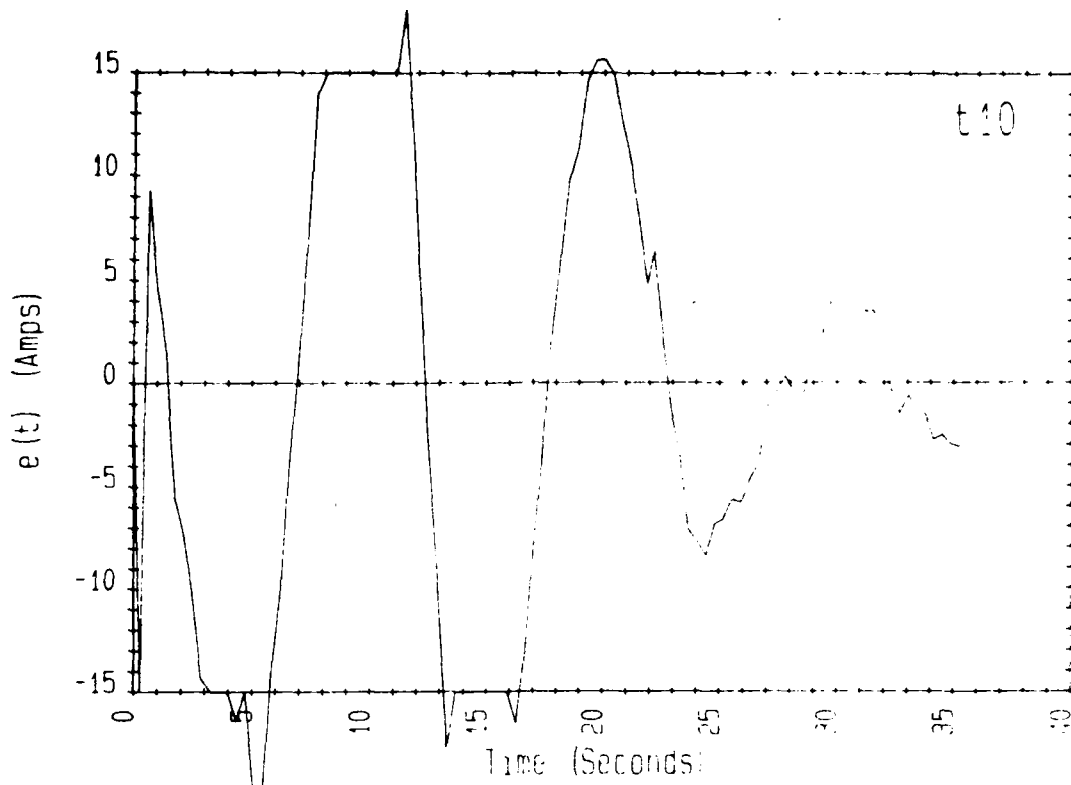


Figure 13. Controller error signal as a function of time for weld T10.

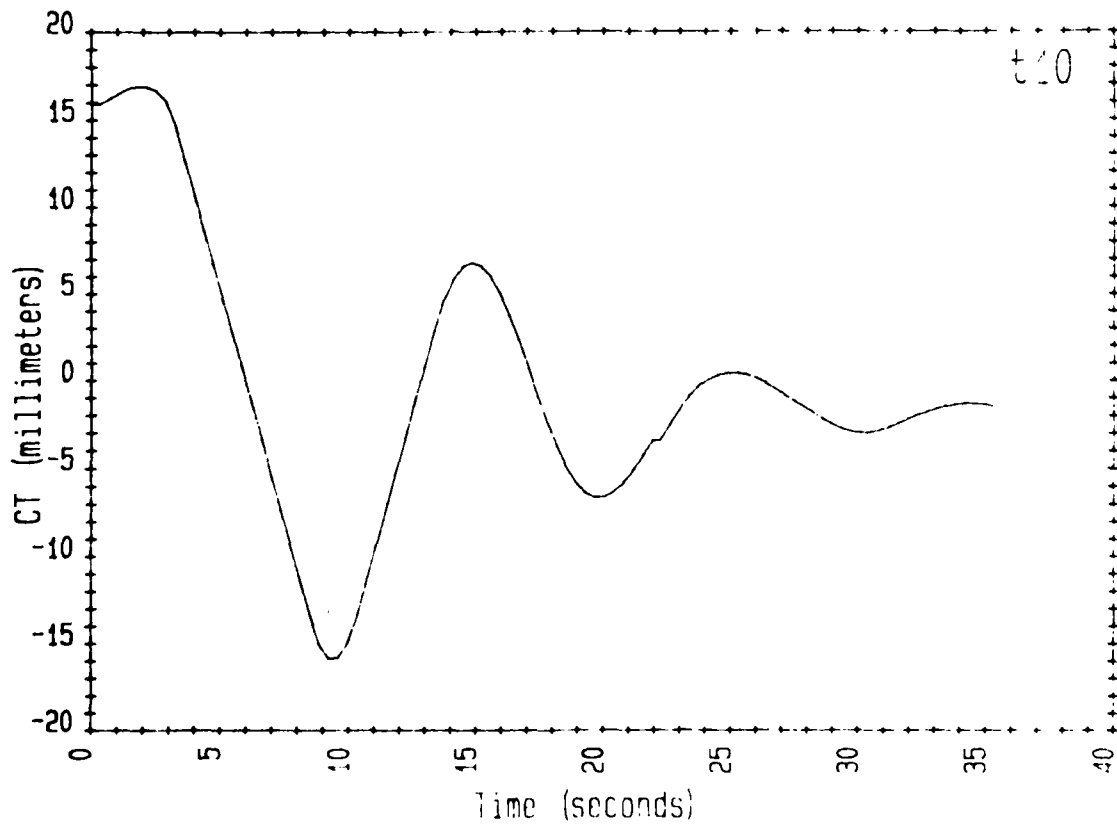


Figure 14. Model-calculated CT as a function of time for weld T10.

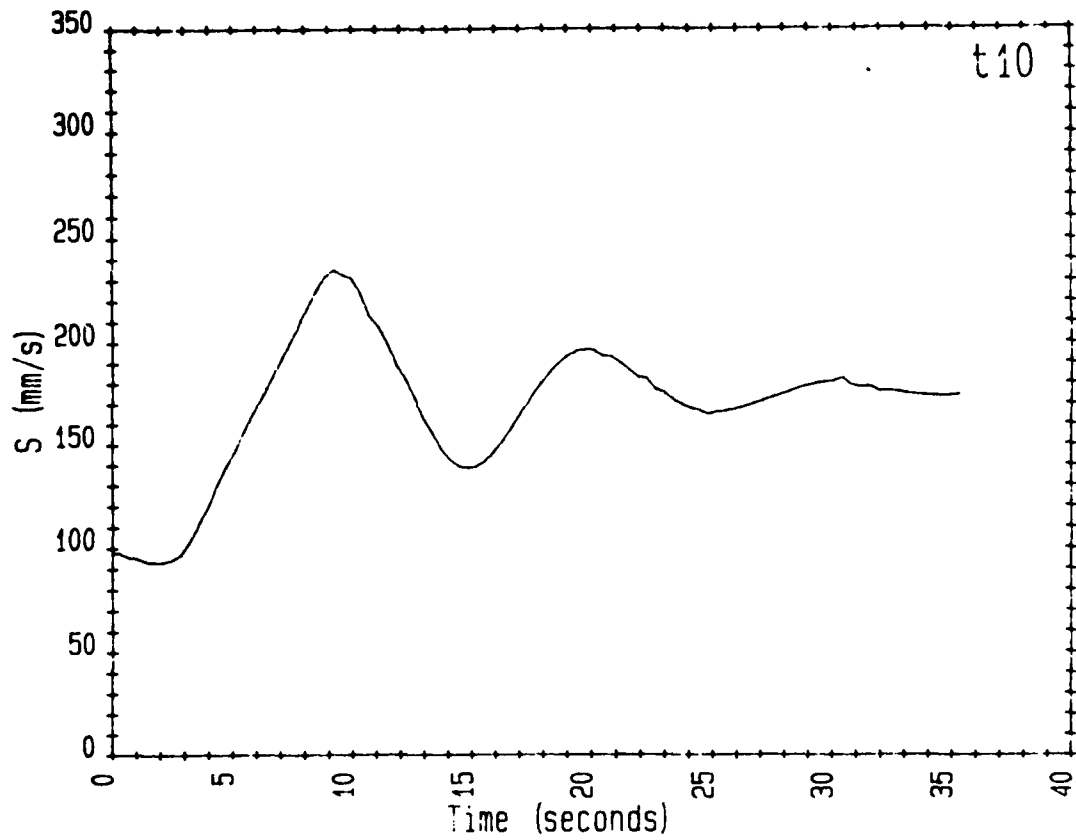


Figure 15. Electrode wire speed as a function of time for weld T10.

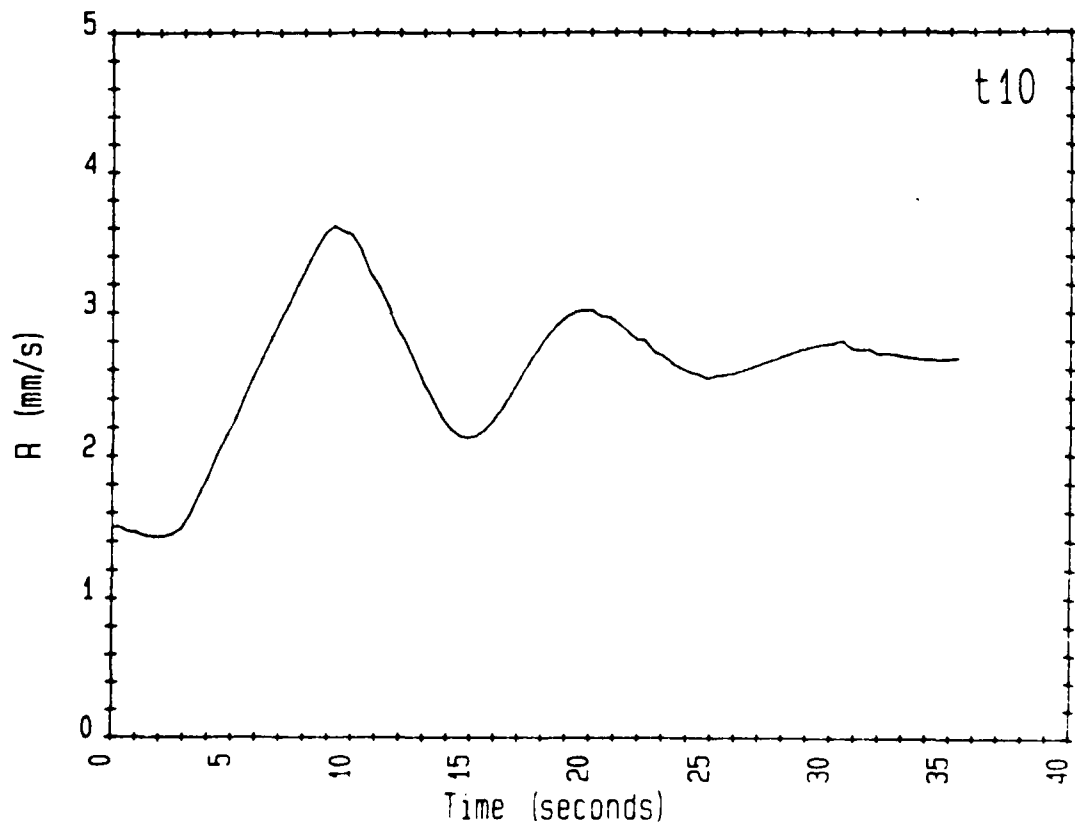


Figure 16. Welding speed as a function of time for weld T10.

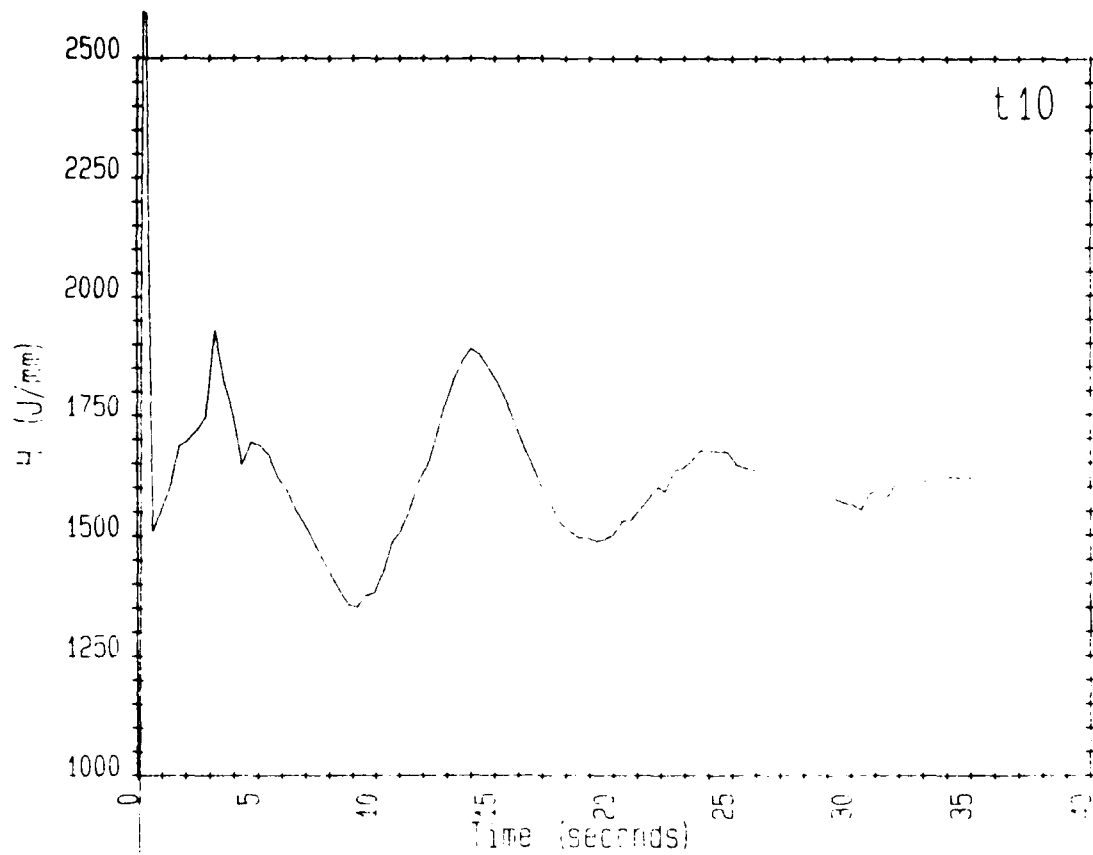


Figure 17. Calculated heat input per length of weld for weld T10.

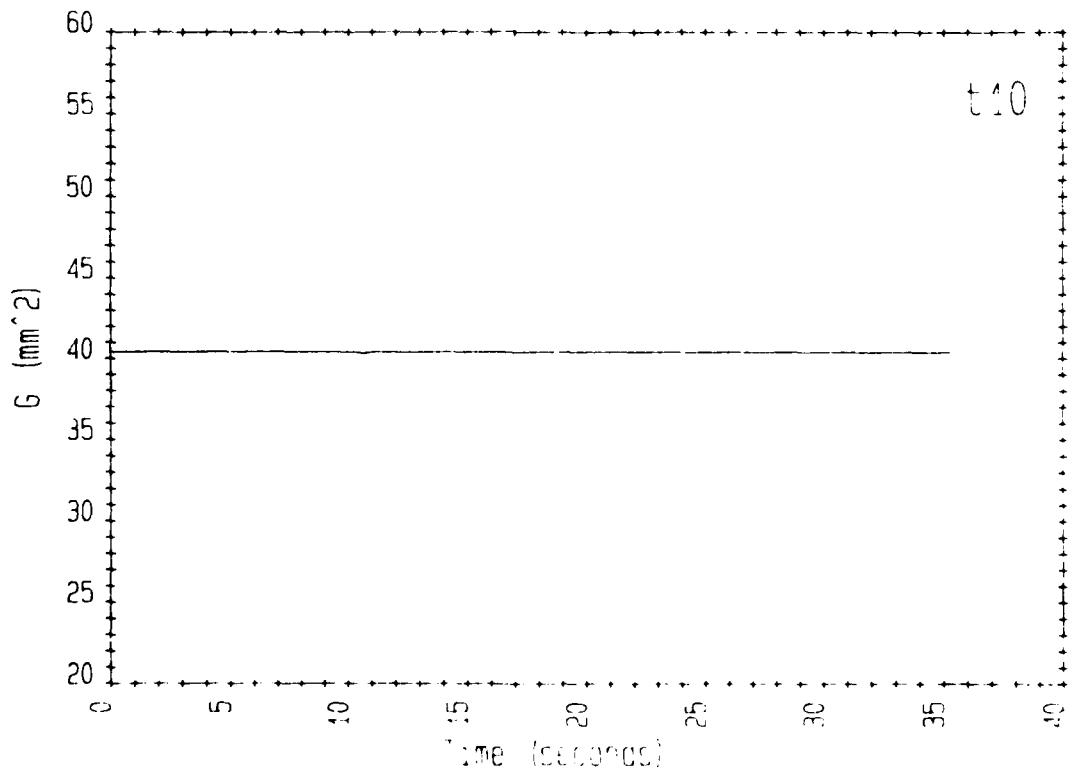


Figure 18. Calculated reinforcement as a function of time for weld T10.

cut-off frequency. In both Figures 9 and 10, data were taken by a separate data acquisition system (Hewlett-Packard model 9000 series 200 computer with an internal ADC) and are limited to the first 11.5 s of welding. In Figure 11, the welding current is shown as measured (filtered) by the welding system computer for the entire weld duration; the model-calculated current is shown in Figure 12. The error signal (e) in Figure 13 is the difference between current values shown in the two previous figures. The resulting controller output, CT, is shown in Figure 14. There is considerable oscillation of CT which decays with time but not fast enough to be of practical value. This results in similar oscillation in the electrode wire speed S (Figure 15) and welding speed R (Figure 16). The heat input per length of weld is shown in Figure 17 and the reinforcement area is shown in Figure 18. The reinforcement area is controlled by ensuring that the ratio of electrode wire speed to weld speed satisfies Equation (9). Consequently, in all the welds the plot of G versus t is similar; the only variations are due to round-off errors. Thus, plots of G versus t are not shown for the following welds.

Figures 19 through 27 illustrate in more detail the behavior of the controller during weld T22. In Figure 19, the weld current is shown, taken at a digitizing rate of 250 Hz; the same data are shown in Figure 20 after having been filtered by a low-pass, first-order Butterworth filter with a 1 Hz cut-off frequency. In Figure 21, the welding current is shown as measured (filtered) by the welding system computer for the entire weld duration; the model-calculated current is shown in Figure 22. The error signal in Figure 23 is the difference between current values shown in the two previous figures. The resulting controller output, CT, is shown in Figure 24. In contrast to the behavior for the earlier weld, CT rapidly (<3 s) approaches its steady-state value. This results in similar, rapid attainment of nominal steady-state values for the electrode wire speed S and welding speed R (Figures 25 and 26). The weld heat input per length of weld is shown in Figure 27.

The use of the computer data acquisition system to obtain welding current values during the first several seconds of welding illustrates the rapid rate at which the electrode wire melting process approaches

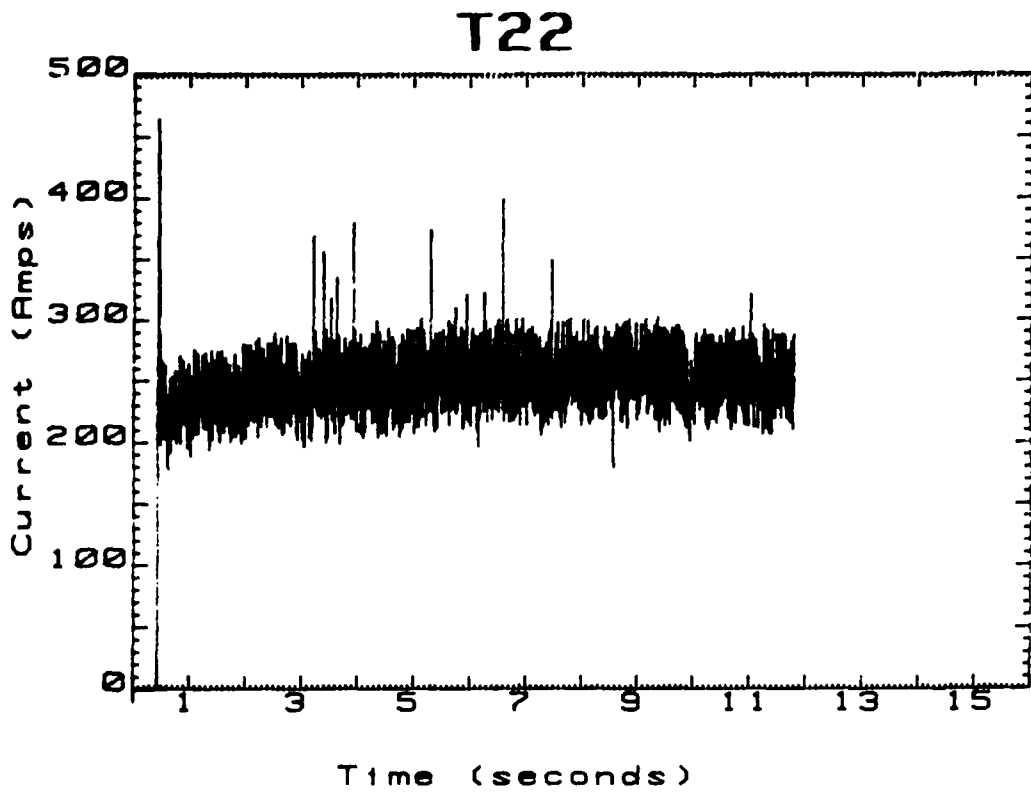


Figure 19. Digitized current as a function of time for weld T22.

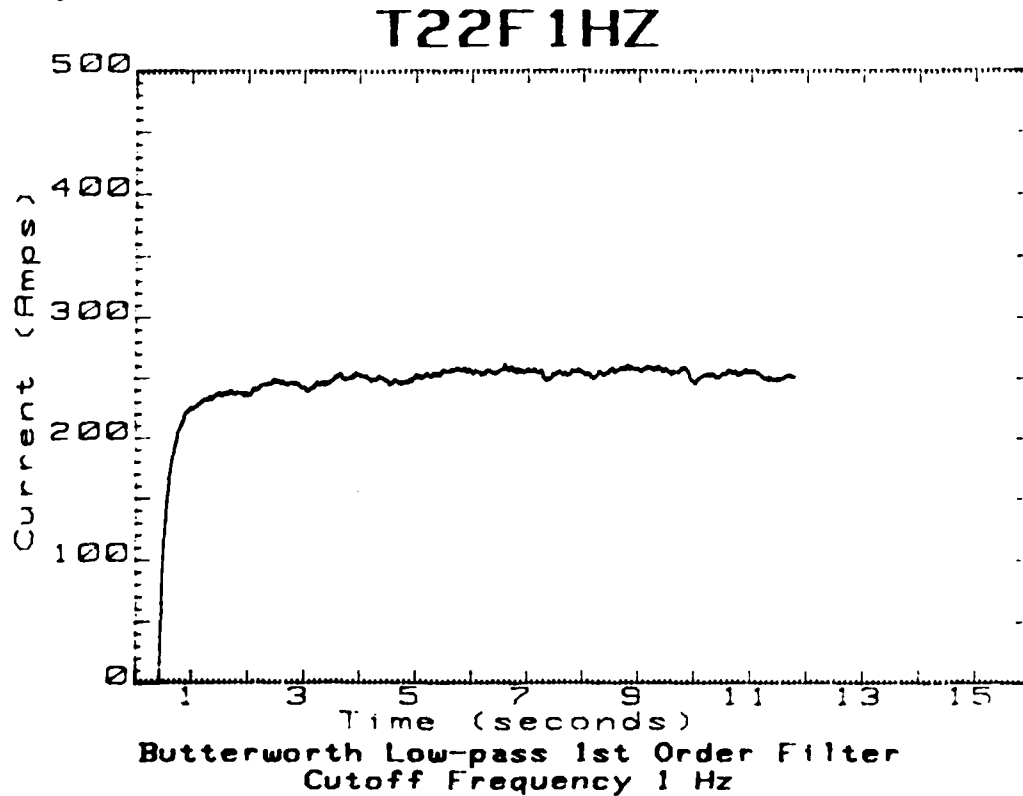


Figure 20. Current as a function of time for weld T22, filtered with a 1 Hz Butterworth low-pass filter.

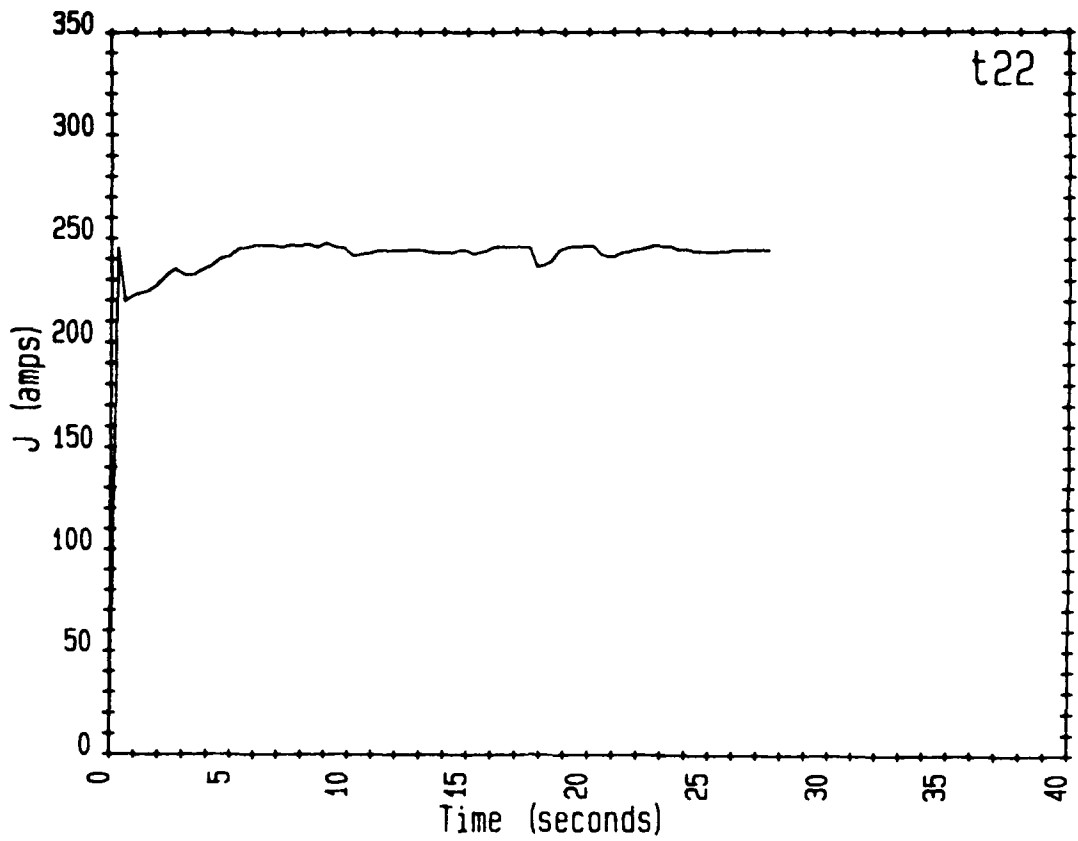


Figure 21. Current as a function of time for weld T22, as measured by the computer-controlled GMA welding machine.

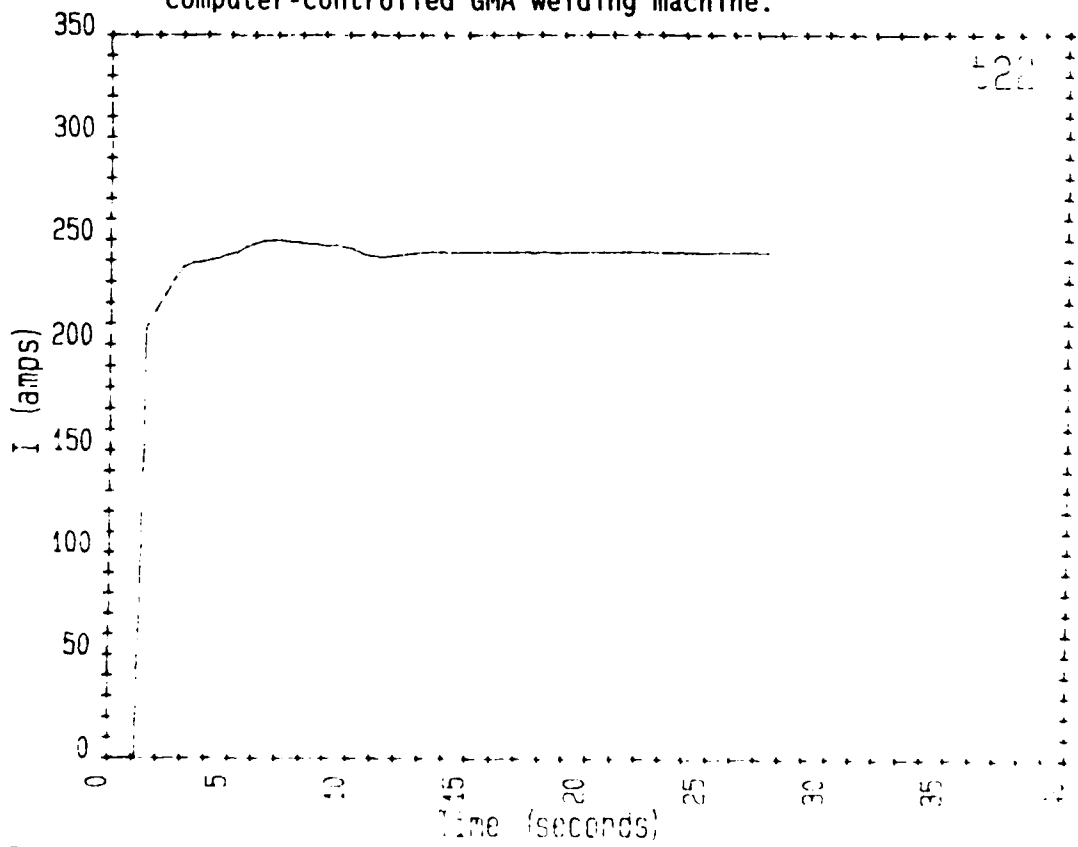


Figure 22. Model-calculated current as a function of time for weld T22.

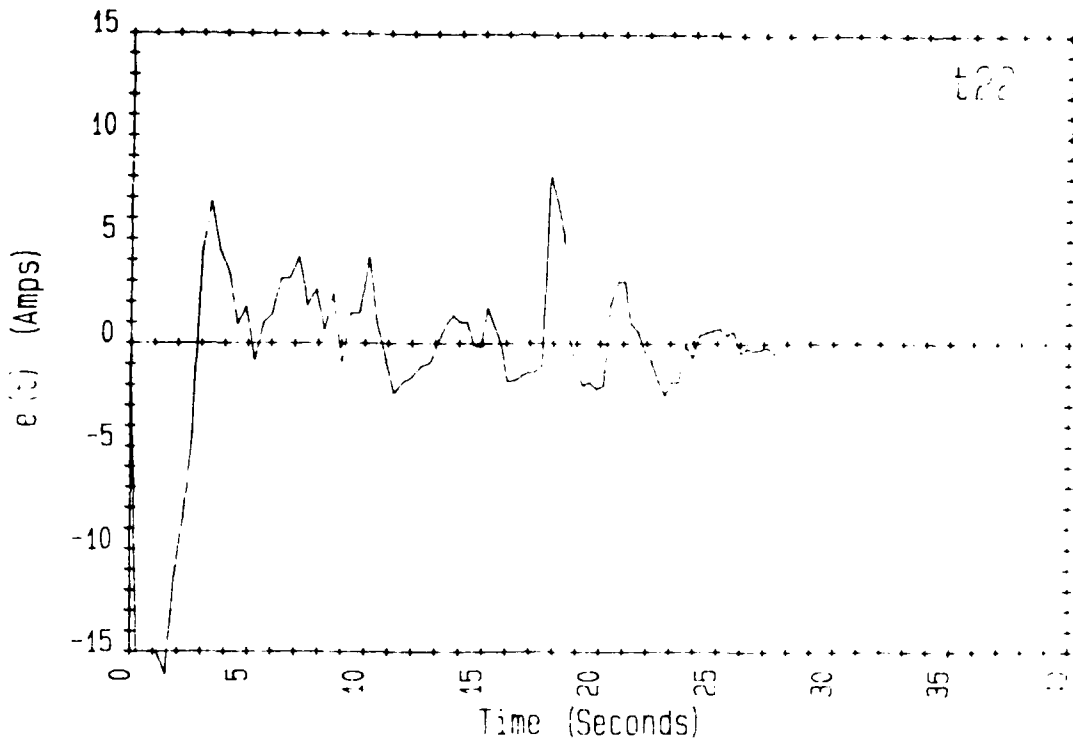


Figure 23. Controller error signal as a function of time for weld T22.

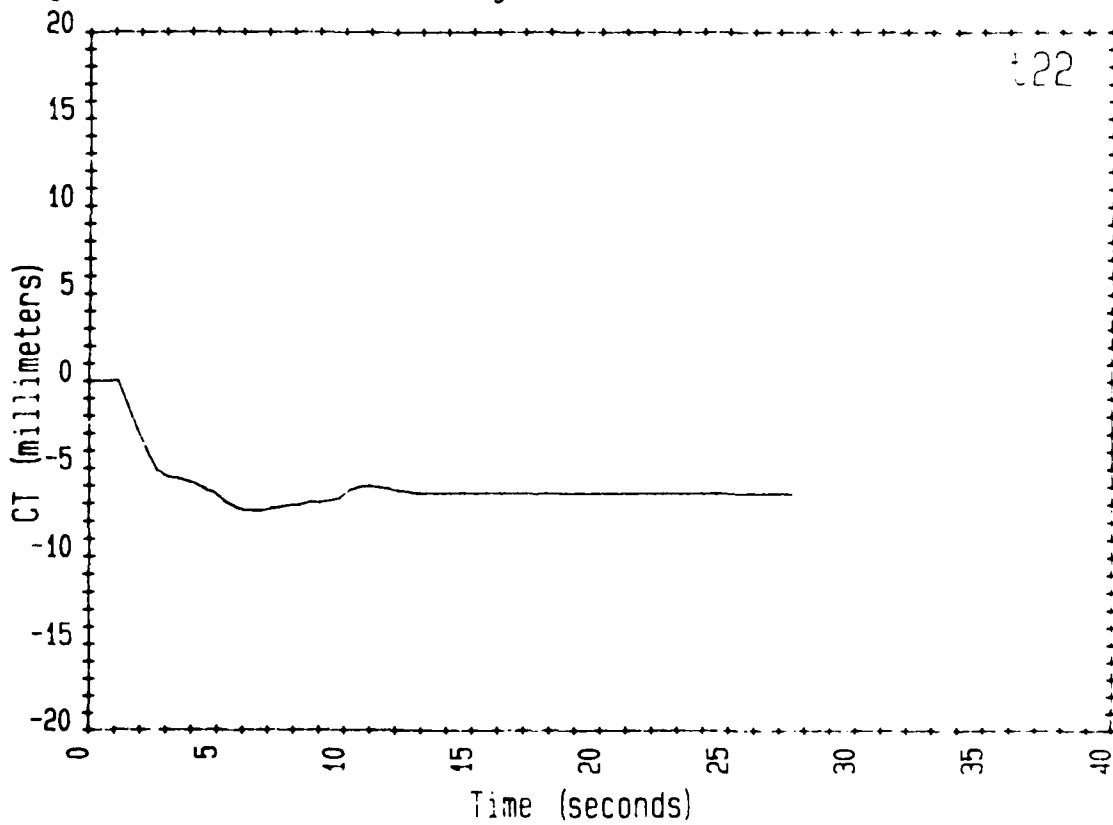


Figure 24. Model-calculated CT as a function of time for weld T22.

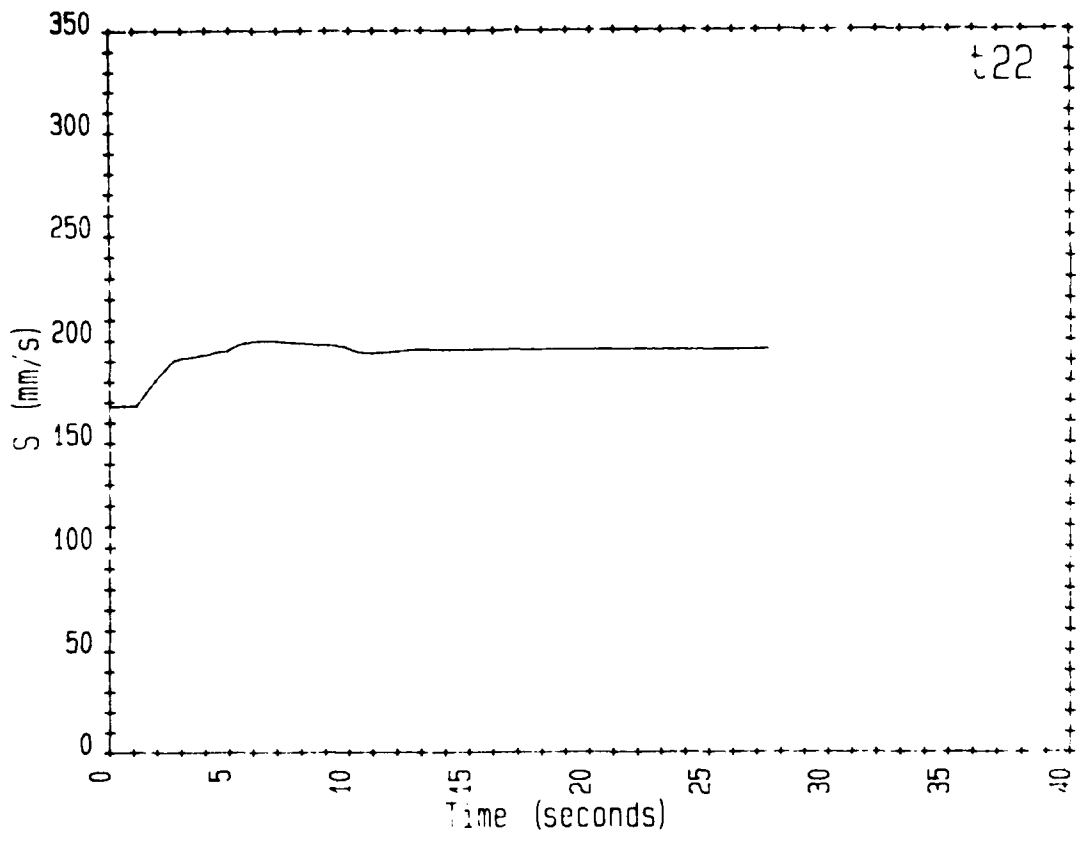


Figure 25. Electrode wire speed as a function of time for weld T22.

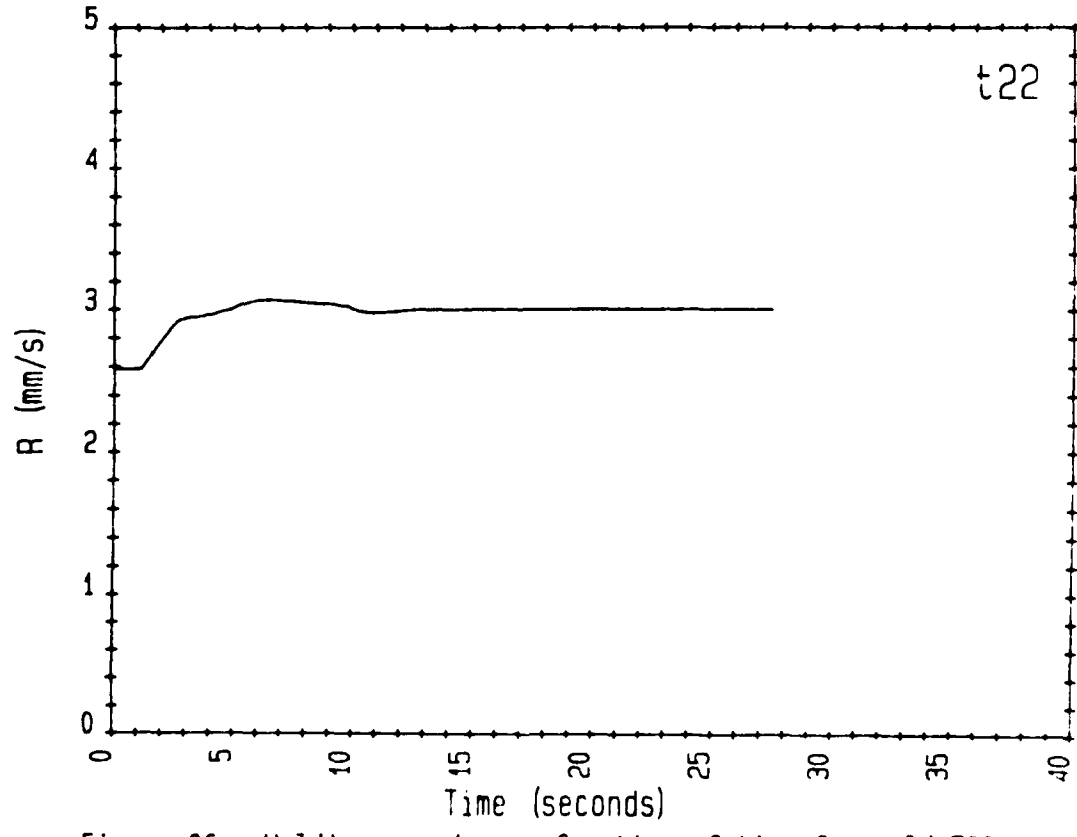


Figure 26. Welding speed as a function of time for weld T22.

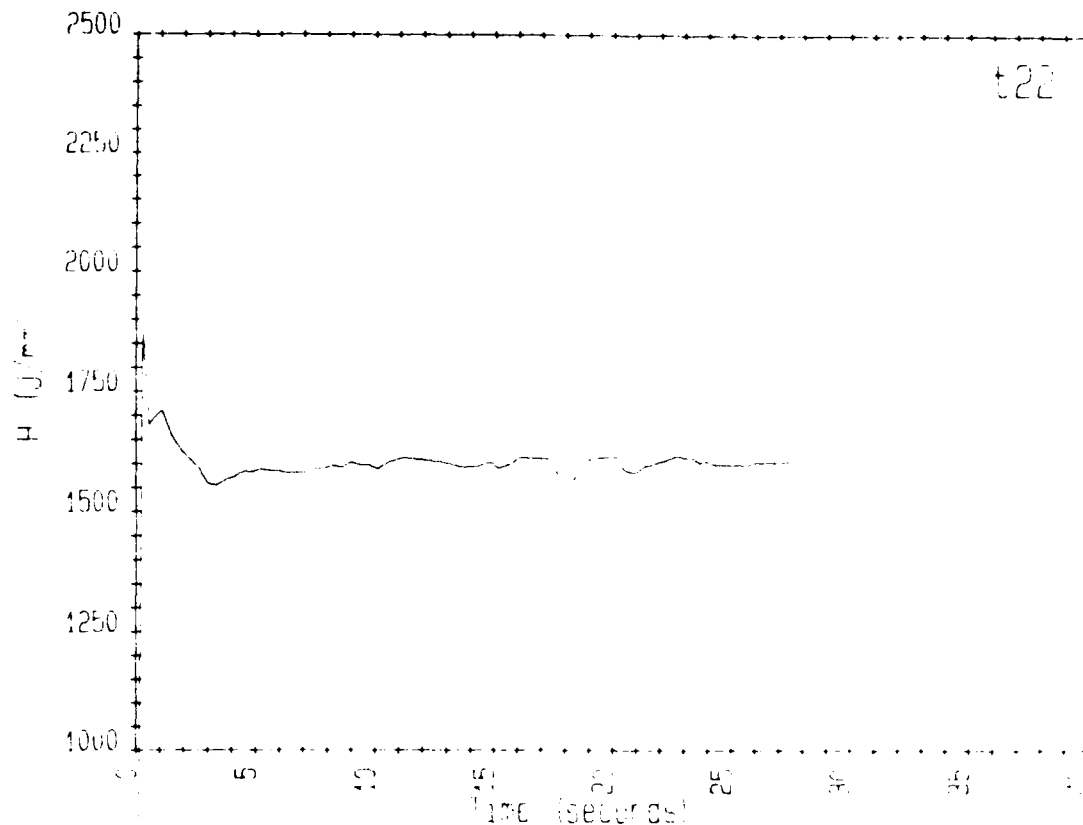


Figure 27. Calculated heat input per length of weld for weld T22.

equilibrium. In Figure 19 it is seen that the current is very close to the steady-state level within probably less than 0.1 s. The apparently slow approach to steady state shown in Figure 8 is due to the fact that strip chart recorders generally function as low-pass filters; indeed it does not require much filtering to introduce error into the data as may be seen by the effect of the 1 Hz low-pass filter in Figure 20, where it apparently has required about 0.5 s for the current to reach nominal steady state. It may be of interest to note that the controller used in this work does not function for the first three program iterations and thus does not operate for the first second of welding. Thus the rapid attainment of nominal steady-state current during startup in weld T22 is due to the fast response of the transistorized power supply. The behavior of the process for times greater than about 1 s is due to the characteristics of the controller. Thus it is realistic to assume in the data which follow that the behavior of the weld bead cooling rate is predominantly a response to the controller dynamics.

Constant Heat Input Cooling Rate

Welds were made at heat inputs of 1480, 1600, and 1800 J/mm and a nominal preheat temperature of 95°F (35°C) with a reinforcement area of 40.4 mm², to determine weld bead cooling rate during startup and at steady state. Open-circuit potential was 27.3 V. Specifically, a thermocouple was inserted into the initial weld pool as soon as possible following initiation of welding, and a second at a distance along the weld bead of ~2 in. following initiation. It was found that the arc was extinguished briefly during thermocouple insertion in many instances, an event which required about 1 s for the arc to restabilize. Such an event is seen in Figure 28, weld T36, at ~7 s into the weld. Consequently data were taken for several welds for each condition. Cooling rates were measured from the slope of compensated thermocouple voltage versus time plots on a HP 7132A strip chart recorder at a temperature of 1000°F.

The heat inputs selected were based on the resulting electrode metal transfer mode. For a reinforcement area of 40.4 mm², a heat input of 1600 J/mm results in a well established spray transfer with a very crisp startup. Increasing the heat input to 1800 J/mm reduces the current and welding speed and results in globular metal transfer. Although it may intuitively seem that increasing the heat input should also increase the current, the opposite is true. As the heat input is decreased to 1480 J/mm, the current and welding speed increase and streaming transfer occurs. The range 1480 to 1800 J/mm is about the maximum, at a reinforcement area of 40.4 mm², over which the process may be used. Although it is possible to weld outside this range, it becomes increasingly difficult to start the process in a stable manner, as discussed later.

Plots of heat input per length are shown for various welds in Figures 29 through 31. In Figure 29, heat input is shown for weld T37 made at a heat input of 1800 J/mm. The variation seen in heat input with time is due to the fact that globular metal transfer occurs at this heat input/reinforcement combination. It may be noted that this weld is similar to that for which Figure 28 was made except that, here, thermocouple insertion did not extinguish the arc. Figure 30 shows the heat input for a

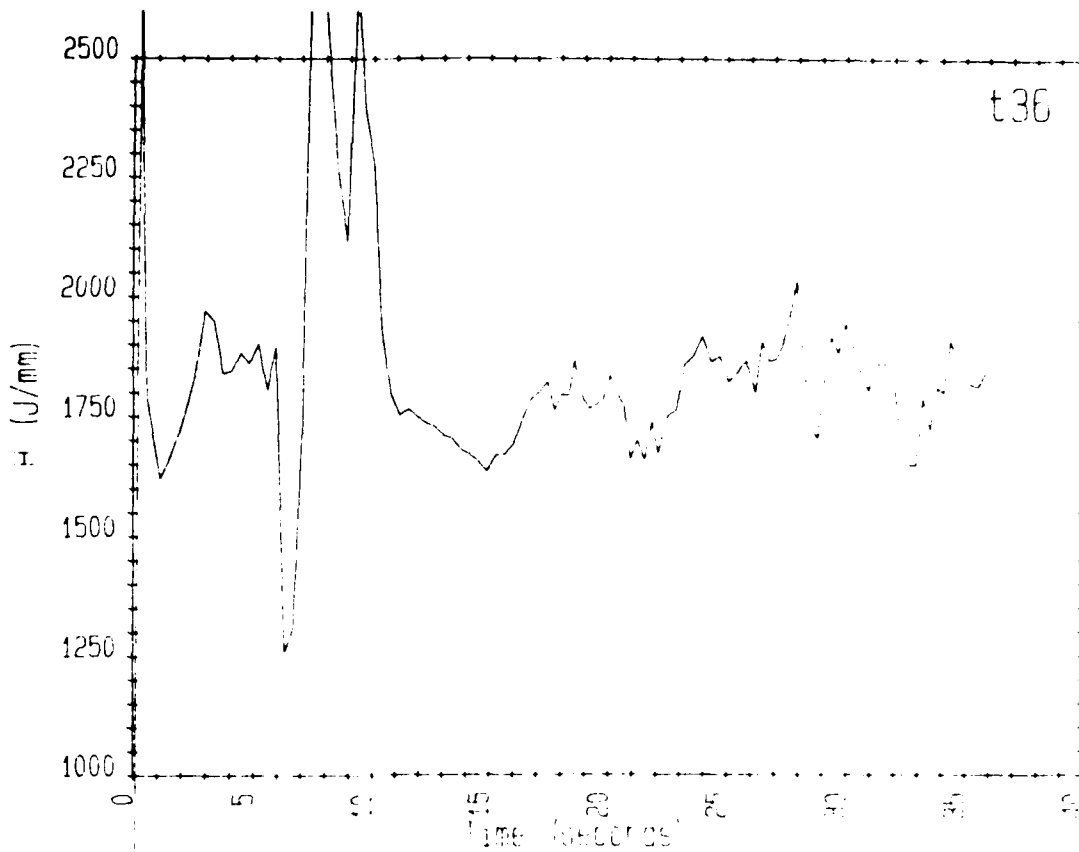


Figure 28. Calculated heat input per length of weld for weld T36.

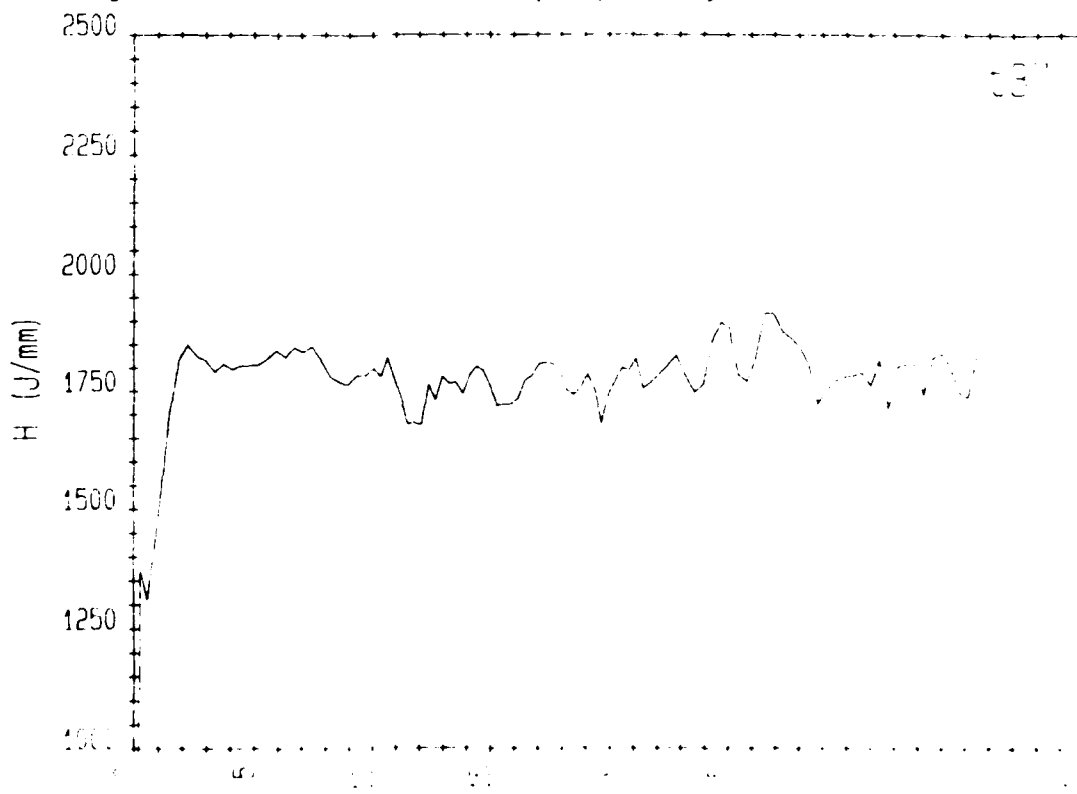


Figure 29. Calculated heat input per length of weld for weld T37.

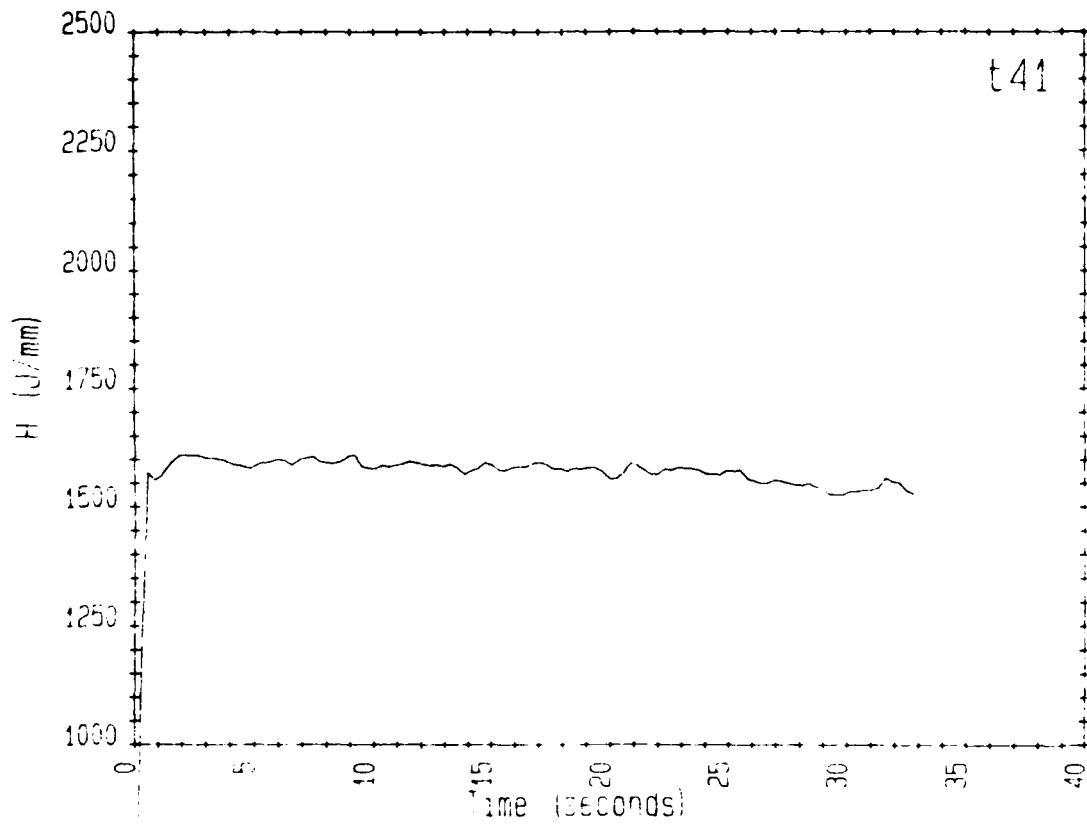


Figure 30. Calculated heat input per length of weld for weld T41.

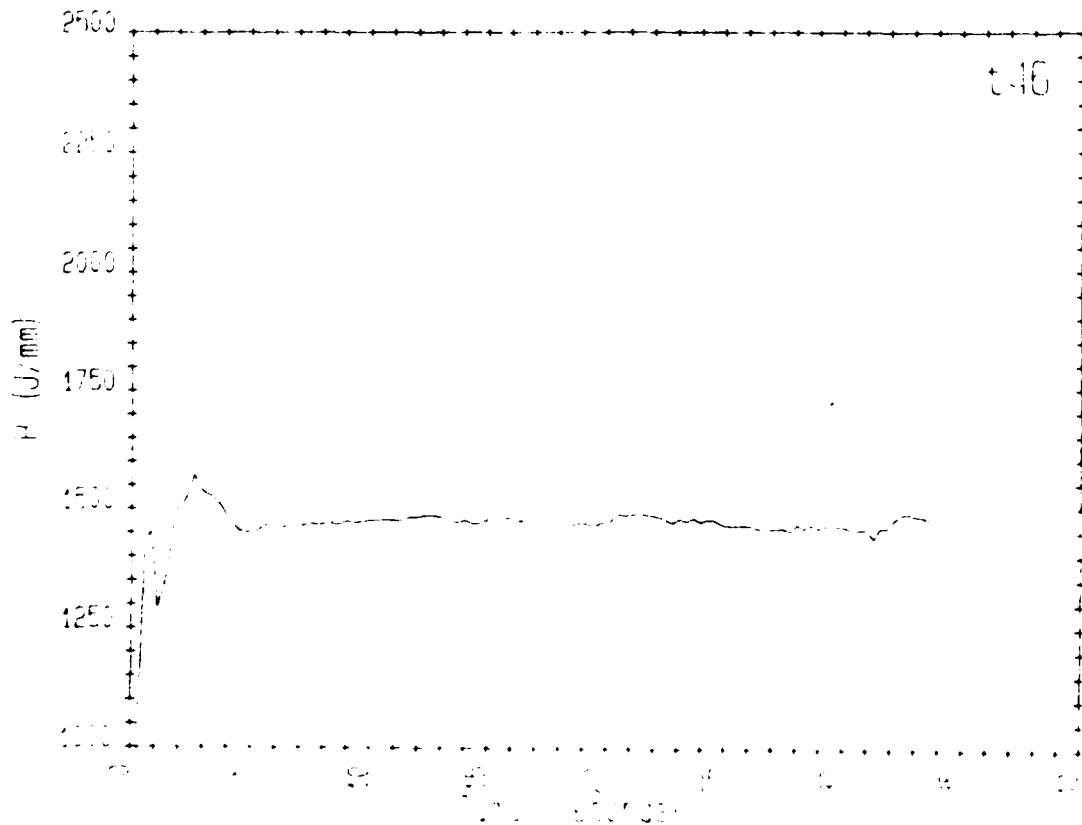


Figure 31. Calculated heat input per length of weld for weld T46.

weld (T41) made at a heat input of 1600 J/mm where spray transfer occurs. Finally, Figure 31 shows heat input for a weld (T46) made at a heat input of 1480 J/mm where streaming transfer occurs.

Cooling rates are plotted in Figure 32 as a function of weld heat input for both the first thermocouple inserted and the second. Inasmuch as thermocouples are difficult to use to obtain good weld bead cooling rate data, the most that can be gathered from the data is that the cooling rate during startup of the process is about a factor of two greater than the cooling rate later in the weld. This is to be expected, as the initial weld bead formed is surrounded by relatively cold base metal; as welding continues, the process effectively preheats the base metal thus reducing the cooling rate.

Stepped Heat Input Cooling Rate

An additional series of welds was made, using a 95°F (35°C) preheat temperature, in which the heat input per length of weld was initially set at 1800 J/mm and then reduced to 1480 J/mm at about 7 s into the weld. Open-circuit potential was 27.3 V. Thermocouples were inserted in the same manner as for the constant heat input welds. The bead reinforcement area was held constant at 40.4 mm² during the entire welds. Figures 33 through 35 show calculated heat input per length of weld determined by the control computer during welding. Globular transfer is occurring during the first 7 s of the three welds, resulting in considerable variation in instantaneous current and thus heat input. Following transfer to the lower heat input, streaming transfer occurs.

Figure 36 shows the measured cooling rates and bead reinforcement areas as a function of position along the weld beads. In this plot the reinforcement areas are measured and show excellent agreement with desired areas. The cooling rate data show results obtained for welds made with a constant heat input (dashed line) and those obtained with a stepped heat input (solid line). The use of a 22% higher initial heat input reduced the initial weld bead cooling rate by ~15%.

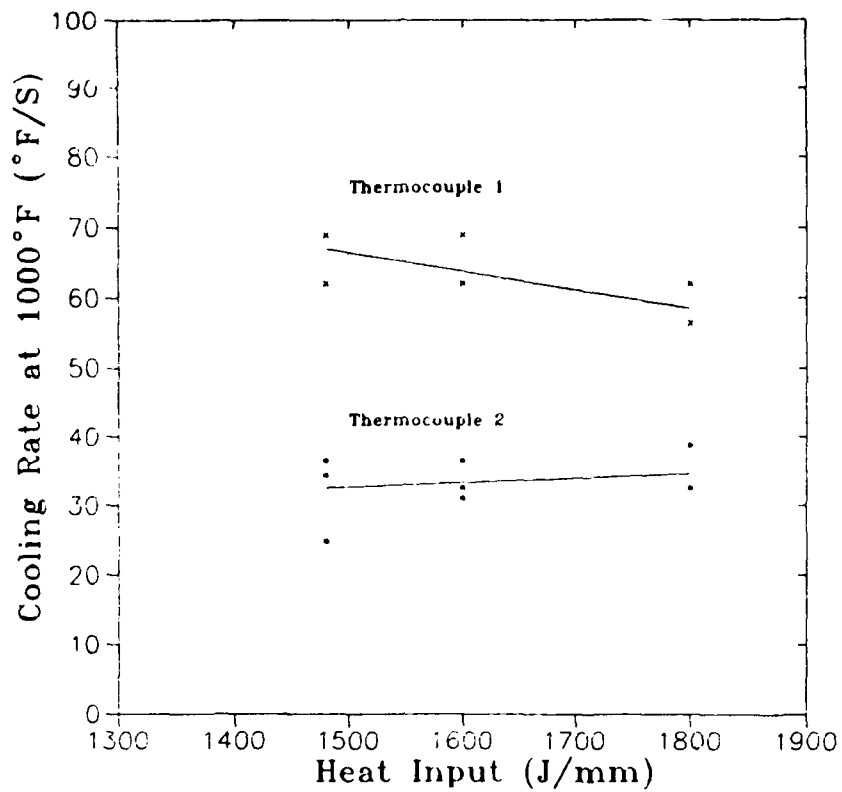


Figure 32. Weld bead cooling rate at 1000°F as a function of heat input per length of weld.

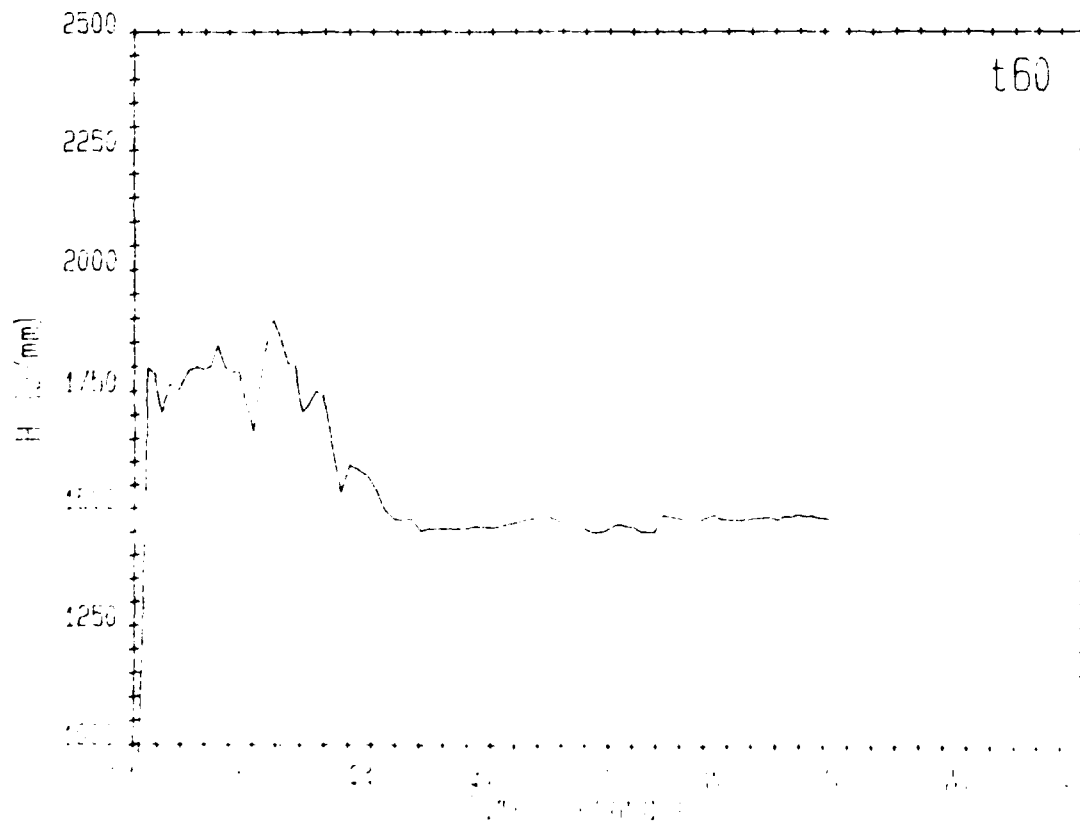


Figure 33. Calculated heat input per length of weld for weld T60.

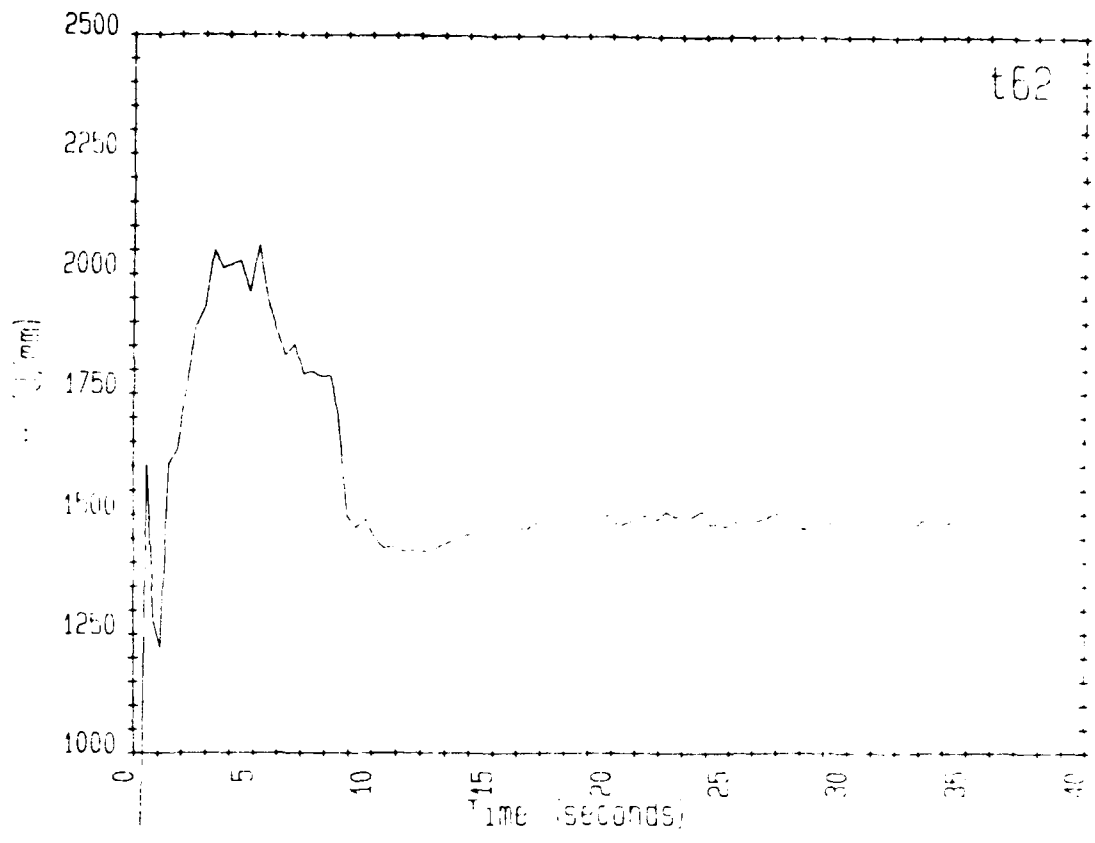


Figure 34. Calculated heat input per length of weld for weld T62.

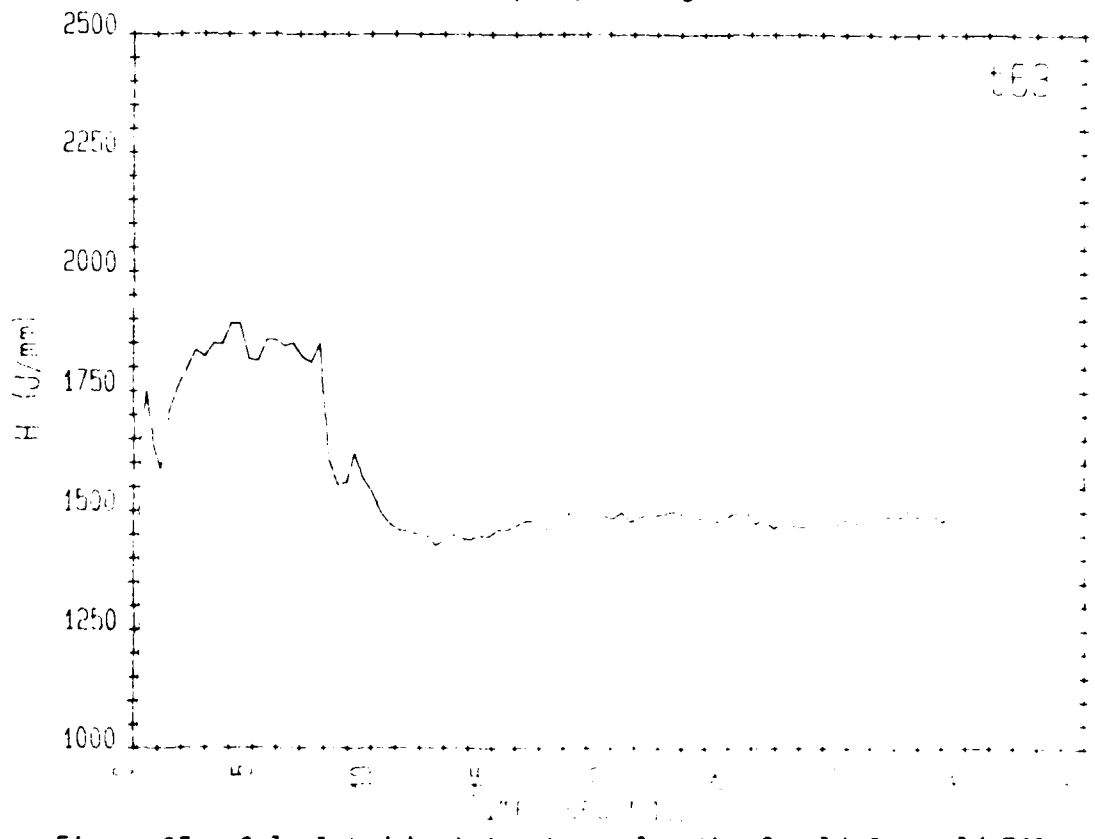
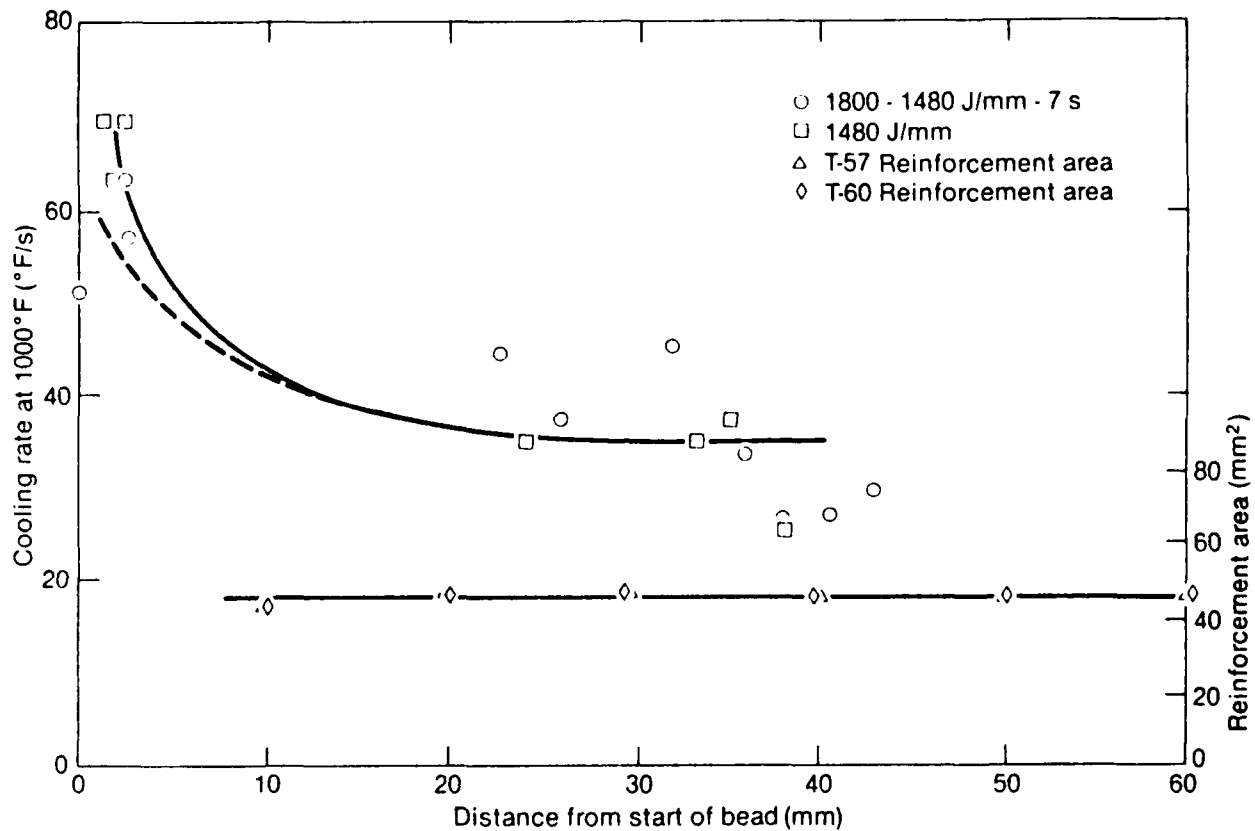


Figure 35. Calculated heat input per length of weld for weld T63.



9-1590

Figure 36. Weld bead cooling rate at 1000°F as a function of distance from start of bead, for 1800/1480 J/mm stepped heat input.

Delayed-Start Stepped Heat Input Cooling Rate

A further series of welds (T64 to T87) was made using a 110°F (41.7°C) preheat temperature and an open-circuit potential of 27.9 V to ensure spray transfer. Again, the initial heat input was set at 1800 J/mm for 7 s, then reduced to 1600 J/mm. At this time, the open-circuit potential was reduced to 27.4 V. Thermocouple placement was the same as in earlier portions of this work. Bead reinforcement was again 40.4 mm².

An additional parameter in making this series of welds was a 4 s programmed delay in starting weld travel. It should be noted that one cannot use the linear heat input designation for this period because the torch has no relative motion. A suitable analogy would be a spot weld at a power level which would correspond to 1800 J/mm for a moving torch.

Spray transfer prevailed throughout the entire welding sequence, although short, minor episodes of globular transfer were seen during the initial 4 s delay.

Figure 37 shows both weld bead cooling rate at 1000°F and weld bead reinforcement area, both as functions of distance from the start of the weld bead. A significant increase in bead reinforcement area can be seen in the first 10 mm of the weld as a consequence of the delayed start. Likewise, the delayed start results in a lower initial cooling rate for the weld bead than was found in previous runs. For these measurements, thermocouple placement appears critical, and we do not yet have a fully quantitative measure of the difference.

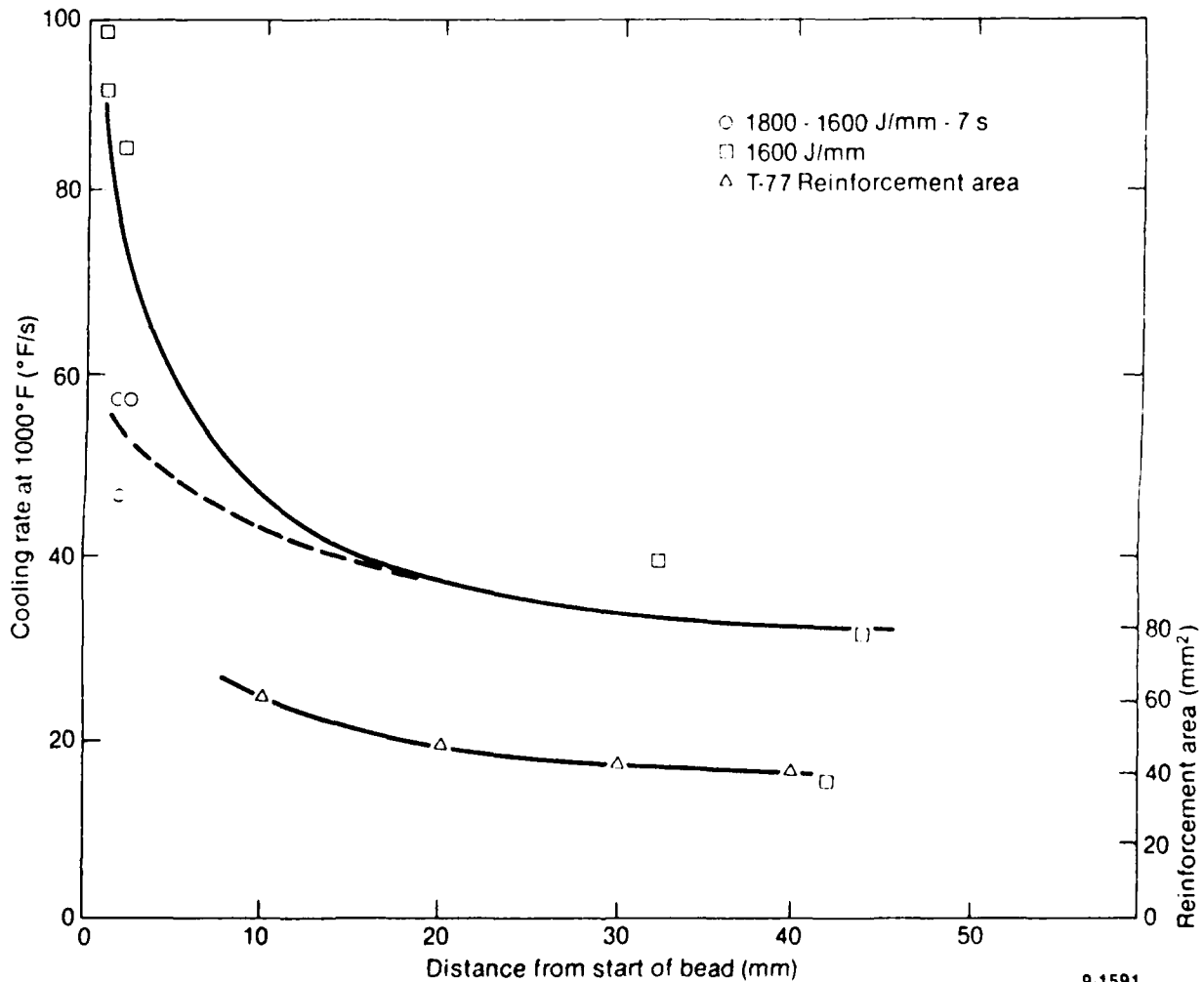


Figure 37. Weld bead cooling rate at 1000°F as a function of distance from start of bead, for 1800/1600 J/mm stepped heat input and 4 s delayed start.

Extrapolation of the 1600 J/mm heat input curve to the start of the weld gives a cooling rate that equals or exceeds 100°F/s, whereas the equivalent delayed stepped heat input value is 60°F/s, a decrease of 40% or more.

Arc Initiation

During startup of the process, the first event which occurs is computer-calculation of the initial value of electrode wire speed, based on the control model. This value is sent to an analog-to-digital converter (ADC) which sends a 0 to 10 V reference signal to the motor power supply. The motor power supply controls the motor speed at the appropriate rate, using feedback from a tachometer. The computer does not calculate a new electrode wire speed value until ~ 1 s following the first value. Thus, the wire is driven down into the base metal at a constant rate. During this time period the welding power supply maintains the electrode at a constant potential (in this case about 28 V) above ground. When the electrode wire contacts the base metal, the welding power supply furnishes current in an attempt to hold the voltage constant. This current melts the electrode wire by resistive heating, and Lorentz forces pinch-off the resulting liquid column, allowing an arc to form. The system rapidly attains a steady-state melting rate equivalent to the wire speed. If the resultant current is within the proper range, the distance from the contact-tip to the end of the electrode wire is some nonzero, positive value less than the contact-tip-to-workpiece distance.

In the above sequence of events, the rate at which the current increases, as the electrode wire contacts the base metal, is critical. If the current increases at too low a rate, the wire either will not melt or the liquid column will not pinch-off and the arc will not form. If the current increases at too great a rate, the arc plasma column will be blown away by the Lorentz forces and the arc either will not form or will require numerous tries before forming. In addition, the steady-state current level must be within the correct range or the arc will transfer to the contact tip or the electrode wire will repeatedly stub into the weld pool. The current level is determined by the control model; the rate at which the current increases is determined by the power supply.

The current required to maintain a given voltage drop is determined by the contact-tip-to-workpiece resistance. For spray transfer with 0.89 mm diameter steel wire, Ar-20₂ shield gas and a current of ~220 A, the total contact-tip-to-workpiece resistance is about 8.1 ohms. This is made up of ~8 ohms wire resistance and 0.1 ohm arc resistance. Thus, changes in the wire resistance are important. Specifically, as molten metal detaches from the electrode wire, its resistance changes rapidly with a resultant effect on the current and melting rate. For example, assuming that the electrical stickout is ~10 mm, in spray transfer the droplets are about the same diameter as the electrode wire; thus, the detachment of a drop reduces the wire electrical stickout by about 9%. This reduction may be expected to correspondingly change the current a similar amount. This effect is important because the instantaneous change in stickout is smaller for spray transfer than for other modes of transfer. (The instantaneous change in stickout may be even smaller for streaming transfer once steady-state operating conditions are reached. However, during arc initiation, the long liquid column present in streaming transfer is subject to pinching-off by the large fluctuation in current and associated Lorentz forces. This behavior frequently leads to rapid swings from stubbing-in to globular transfer.)

The current variations experienced during arc initiation are at a minimum for conditions corresponding to steady-state spray transfer. Thus, the startup of the process is smoother and the electrode wire attains steady-state operating conditions faster. This may be seen in Figure 30, for a weld made at a heat input of 1600 J/mm with steady-state spray transfer, where the process attains steady-state operating conditions in well under one second. In contrast, for welds made with globular transfer (Figure 29) and streaming transfer (Figure 31) 2 to 3 s are required for the process to attain nominal steady-state operating conditions.

The rate of change in the current from the power supply may be limited by altering the power supply and secondary (welding) circuit inductance. The greater the inductance, the less extreme the variation in current with time. Thus, increasing the inductance allows smoother arc starts to be made over a wider range of initial electrode wire speeds. Older style power

supplies frequently incorporated a variable inductor as part of the system. The transistor regulator in the power supply used in this work has a very low, fixed inductance. But it does employ a feedback circuit which monitors the actual voltage and controls the rate at which the power supply voltage changes (up to the 40 kHz response frequency). Provision is made to change the effective inductance of the power supply by altering the characteristics of the feedback circuit. Experience has shown that increasing the inductance (I_b) setting on the power supply to a maximum of nine significantly improves arc initiation under conditions which would otherwise result in poor starts.

Even with the effective power supply inductance increased, arc starts are still smoother for conditions corresponding to steady-state spray transfer. In a computer-controlled welding system, such as used in this work, it is possible to exploit this characteristic. Arc starts may be made at conditions which correspond to steady-state spray transfer. The current may be rapidly changed to a level outside the range at which spray transfer occurs. For example, in this work, the arc may be started at a heat input of 1600 J/mm, changed to 2000 J/mm (or higher) at one second, held at that level for 6 to 7 s and then reduced to 1480 J/mm for the duration of the weld.

RESULTS AND CONCLUSIONS

Although the range of values included in this study is limited, it is clear that the weld bead cooling rate during startup of the process may be significantly reduced by increasing the heat input to the weld while maintaining a constant mass input. Increasing local mass input (by delaying the start of weld movement) further reduces the initial cooling rate through its heat contribution. It is recognized that larger changes in heat input than were used in this work are needed. The factors which influence arc initiation have been discussed, and the manner in which this knowledge may be used to allow greater ranges in heat input to be used while obtaining smooth arc starts has been considered.

It is possible to expand the spray transfer operating range by increasing the process operating voltage. It is also possible to alter the position of the spray transfer region in the heat input/reinforcement domain by changing the contact-tip-to-workpiece distance. Thus it is possible that simultaneous changes in the voltage and torch-to-workpiece distance will allow larger differences in heat input to be obtained.

In summary:

1. A steady-state model of GMA wire melting and base-metal heat and mass inputs has been successfully applied to the problem of independently controlling weld heat and mass input.
2. A proportional-integral controller has been developed and controller gains determined to allow stable operation during globular, spray, and streaming transfer modes.
3. The above controller has been used to decrease the initial weld bead cooling rate by applying a relatively high heat input during the first several seconds of the weld and then decreasing the heat input to a lower steady-state value while maintaining a constant

reinforcement area. Further reduction of the initial cooling rate has been achieved by incorporating a brief delay in starting weld travel into the weld startup program.

4. The influences of steady-state metal transfer mode and power supply effective inductance on arc start have been discussed. Arc starts are smoother during conditions corresponding to steady-state spray transfer and with higher levels of effective power supply inductance.
5. Starting the process at heat input levels corresponding to spray transfer and then rapidly changing to higher levels before reducing to the nominal level required for the weld should result in additional reduction in initial weld bead cooling rates.

The present work demonstrates the feasibility of modifying the initial weld bead cooling rate by increasing the initial heat input and changing the initial weld procedure program. The results also make it clear that achievement of the optimum condition, equal initial and steady-state cooling rates, is practicable only with a supplemental heat source.

REFERENCES

1. R. L. Ule, "A Study of the Thermal Profiles During Autogenous Arc Welding," M.S. Thesis, Naval Postgraduate School, Monterey, CA, March 1989.
2. H. B. Smartt, J. A. Johnson, R. A. Morris, A Machine Design and Process Control Concept for Automated Arc Welding, EGG-MS-7842, September 1987.
3. J. F. Lancaster, "Metal Transfer and Mass Flow in the Weld Pool," The Physics of Welding, J. F. Lancaster (ed.), New York: Pergamon Press, 1984, pp. 204-267.
4. J. H. Waszink and M. J. Piena, "Experimental Investigation of Drop Detachment and Drop Velocity in GMAW," Welding Journal, 1986, pp. 289-s to 298-s.
5. K. G. Beauchamp and C. K. Yuen, Digital Methods for Signal Analysis, London: George Allen & Unwin, 1979.